Masterarbeit

Subhangee Sahoo

Integration of Tactile & Visual Feedback for Guidance in Hollow Organs

LEHRSTUHL FÜR MEDIZINISCHE INFORMATIONSTECHNIK

Fakultät für Elektrotechnik und Informationstechnik, RWTH Aachen

Univ.-Prof. Dr.-Ing. Dr. med. Dr. h.c. Steffen Leonhardt

Betreuer-/in: Ms. Laura Oliva Maza (Deutsches Zentrum für Luft- und Raumfahrt (DLR) Oberpfaffenhofen) & Dr.-Ing. Markus Lüken

Datum: 10. Dezember 2025

Acknowledgement

I would like to express my sincere gratitude to my supervisors, Ms. Laura Oliva Maza and Dr.-Ing. Markus Lüken, for their invaluable guidance, continuous support, and insightful feedback throughout the course of this thesis. Their expertise and encouragement greatly contributed to the depth and direction of this research.

I am equally grateful to Prof. Dr. H.C. Steffen Leonhardt from MedIT, RWTH, and Prof. Dr. Rudolph Triebel & Dipl. Ing. Julian Klodmann from Deutsches Zentrum für Luft- und Raumfahrt (DLR) Oberpfaffenhofen, for providing technical insights, resources, and constructive discussions that helped shape this work.

I am grateful to the members of the Surgical Robotics team of DLR Oberpfaffenhofen, particularly Mr. Florian Steidle, Mr. Michael Dyck, Mr. Alexander Kirst and Ms. Dorothea Brackenhammer, for their assistance with hardware and software components, planning the experimental setups and Mr. Bernhard Weber for the help with the exploratory study and the data analysis.

Additionally, I would like to acknowledge the support of Dr.-Ing. Thomas Hulin and Mr. Ajithkumar Narayanan Manaparampil for their support with technical modules which were crucial for the completion of this thesis.

I would like to extend my appreciation to my colleagues at DLR, including Dr. Neal Y. Lii, for their collaborative spirit, discussions, and for creating a stimulating and collaborative research environment. Their assistance during experiments, reviews, and technical troubleshooting has been immensely helpful.

This work benefited from the generous support of several external partners. I would like to acknowledge the provision of FingerTac, the tactile module, developed under the Centre for Tactile Internet with Human-in-the-Loop (CeTI), Funded by the German Research Foundation (DFG, Deutsche Forschungsgemeinschaft) as part of Germany's Excellence Strategy – EXC 2050/1 – Project ID 390696704 – Cluster of Excellence "Centre for Tactile Internet with Human-in-the-Loop" (CeTI) of Technische Universität Dresden, an important module used in this thesis. I also extend my thanks to ImFusion GmbH for granting access to the graphical user interface, ImFusion Suite, which greatly facilitated the visualization.

My special thanks go to my colleagues and friends for their moral support, patience, and companionship during this journey. I am also deeply thankful to my family for their unwavering love, understanding, and encouragement throughout my studies.

I am also grateful to the Scholarship for Completing Studies for International Students, awarded by RWTH Aachen through the DAAD's STIBET I program, funded by the German Federal Foreign Office, for granting partial financial support during the thesis.

Zentrales Prüfungsamt/Central Examination Office

Eidesstattliche Versicherung
Declaration of Academic Integrity

______________________________ ______________________________

Name, Vorname/Last Name, First Name

Matrikelnummer (freiwillige Angabe)
Student ID Number (optional)

Ich versichere hiermit an Eides Statt, dass ich die vorliegende Arbeit/Bachelorarbeit/ Masterarbeit* mit dem Titel
I hereby declare under penalty of perjury that I have completed the present paper/bachelor's thesis/master's thesis* entitled

selbstständig und ohne unzulässige fremde Hilfe (insbes. akademisches Ghostwriting) erbracht habe. Ich habe keine anderen als die angegebenen Quellen und Hilfsmittel benutzt; dies umfasst insbesondere auch Software und Dienste zur Sprach-, Text- und Medienproduktion. Ich erkläre, dass für den Fall, dass die Arbeit in unterschiedlichen Formen eingereicht wird (z.B. elektronisch, gedruckt, geplottet, auf einem Datenträger) alle eingereichten Versionen vollständig übereinstimmen. Die Arbeit hat in gleicher oder ähnlicher Form noch keiner Prüfungsbehörde vorgelegen.
independently and without unauthorized assistance from third parties (in particular academic ghostwriting. I have not used any other sources or aids than those indicated; this includes in particular software and services for language, text, and media production. In the event that the work is submitted in different formats (e.g. electronically, printed, plotted, on a data carrier), I declare that all the submitted versions are fully identical. I have not previously submitted this work, either in the same or a similar form to an examination body.

Ort, Datum/City, Date

Unterschrift/Signature

*Nichtzutreffendes bitte streichen/Please delete as appropriate

Belehrung:
Official Notification:

§ 156 StGB: Falsche Versicherung an Eides Statt
Wer vor einer zur Abnahme einer Versicherung an Eides Statt zuständigen Behörde eine solche Versicherung falsch abgibt oder unter Berufung auf eine solche Versicherung falsch aussagt, wird mit Freiheitsstrafe bis zu drei Jahren oder mit Geldstrafe bestraft.
§ 156 StGB (German Criminal Code): False Unsworn Declarations
Whosoever before a public authority competent to administer unsworn declarations (including Declarations of Academic Integrity) falsely submits such a declaration or falsely testifies while referring to such a declaration shall be liable to imprisonment for a term not exceeding three years or to a fine.
§ 161 StGB: Fahrlässiger Falscheid; fahrlässige falsche Versicherung an Eides Statt
(1) Wenn eine der in den §§ 154 bis 156 bezeichneten Handlungen aus Fahrlässigkeit begangen worden ist, so tritt Freiheitsstrafe bis zu einem Jahr oder Geldstrafe ein.
(2) Straflosigkeit tritt ein, wenn der Täter die falsche Angabe rechtzeitig berichtigt. Die Vorschriften des § 158 Abs. 2 und 3 gelten entsprechend.
§ 161 StGB (German Criminal Code): False Unsworn Declarations Due to Negligence
(1) If an individual commits one of the offenses listed in §§ 154 to 156 due to negligence, they are liable to imprisonment for a term not exceeding one year or to a fine.
(2) The offender shall be exempt from liability if they correct their false testimony in time. The provisions of § 158 (2) and (3) shall apply accordingly.

Die vorstehende Belehrung habe ich zur Kenntnis genommen:
I have read and understood the above official notification:

Ort, Datum/City, Date

Unterschrift/Signature

Summary

Robotic systems have increasingly become integral to modern surgery, with significant advances in assistive technologies enhancing the precision and safety of minimally invasive procedures. Historically, until the 1990s, most major urological surgeries, were performed through open approaches. With the advent of surgical robotics in the early 2000s, their application in urology has expanded rapidly, particularly in endourological procedures aimed at improving surgical outcomes and reducing patient recovery time, such as kidney stone removal. Ureteroscopy (URS) is an endoscopic technique used for the visualization and treatment of the ureter, and in some cases, the renal pelvis, by introducing a rigid or semirigid ureteroscope retrogradely through the urethra and bladder. When performed using a flexible ureteroscope, the procedure is referred to as flexible ureteroscopy (fURS).

This thesis aims to enhance the assistance robotics can provide during fURS, as plug-and-play solutions, particularly to improve navigation within the renal collecting system, minimize collisions with the walls of the kidney, and facilitate efficient trajectories to kidney stones for inspection or removal. The primary goal involves providing an additional bird's eye view of the kidney, which eliminates the limited localization inside the human body, that surgeons face with the endoscopic camera feed. This view gives the real-time tracking of the ureteroscopic endoscope's tip location inside the renal collecting system and helps the surgeon understand which areas have been already monitored, which portion has the stone(s) or need further examination.

A second visual feedback system will project pre-defined trajectories from the entrance to the stones, which can help the surgeons navigate in a quicker and safer manner. Current state-of-the-art systems achieve this through real-time 3D reconstruction of intraoperative endoscopic video, using structure from motion or Simultaneous Localization and Mapping (SLAM) algorithms, or by fusing pre-operative imaging data such as CT or MRI with live intraoperative feeds to create augmented reality (AR) overlays.

Another goal is to integrate tactile feedback to alert the surgeon in critical scenarios, like unintended collisions with the tissues or deviations from the desired trajectory beyond a desired threshold value. Recent commercial devices provide surgeon-side kinesthetic/force cues, while research systems add intra-instrument force/torque sensing, tip pressure sensing, and vibrotactile or audio cues for grasp safety and collision avoidance. This thesis introduce a vibration-based feedback module to alert the surgeon, with user-defined vibration strength and trigger conditions.

The different feedback methodologies introduced in this thesis are designed to be modular and system-agnostic, allowing seamless integration with existing robotic or endoscopic platforms without the need for significant computational overhead. This thesis collectively aims to enhance spatial awareness, reduce procedural errors, and ultimately shorten the learning curve for complex minimally invasive surgeries.

Inhaltsverzeichnis

Symbol directory

Abbreviations

em	electromagnetic
RAS	Robot-assisted surgery
URS	Ureteroscopy
fURS	flexible-Ureteroscopy
DLR	Deutsches Zentrum für Luft- und Raumfahrt, Oberpfaffenhofen
SLAM	Simultaneous Localization and Mapping
CT	Computed Tomography scans
3D	three dimensional
MRI	Magnetic Resonance Imaging

1 Introduction

Over the past two decades, assistive systems have become integral to modern surgical practice, particularly in minimally invasive surgery (MIS), where visibility, dexterity, and precision are inherently limited. Surgical platforms exemplify how robot-assisted surgery can enhance precision, reduce invasiveness and blood loss, and shorten hospital stay compared with open surgery, contributing to improved perioperative outcomes across several specialties [PNL+24].

Building on these advances, computer-assisted and image-guided surgery (IGS) systems further extend surgical capabilities by providing real-time navigation and visualization by fusing preoperative and intraoperative imaging with instrument tracking. These platforms allow surgeons to localize instruments in complex anatomical regions with millimetric accuracy, improving safety and confidence in confined or anatomically variable workspaces [LLY23], [KPL13].

Haptic and tactile feedback systems are being developed to compensate for the loss of direct touch inherent to MIS. Experimental and early clinical studies show that restoring force or tactile cues can reduce applied forces, improve accuracy, and lower task completion times in robot-assisted procedures [Oka09], [BFW23], [SDA24].

Together, these assistive systems - robotic platforms, navigation technologies, and haptic interface are transitioning from passive instruments to active collaborators that enhance situational awareness, standardize performance, and ultimately aim to improve patient outcomes while reducing surgeon workload and cognitive burden [DK24], [MRK+24].

Advantages of assisted surgeries: [Oka04]

- Minimally invasive approach: The incisions are smaller, resulting in reduced trauma to the tissue, less blood loss and reduced post-surgery complications. This also helps cut down the total duration of surgery and faster healing for the patient. [NGBS+23] [GBB+11]
- Enhanced instrument articulation (e.g., “wristed” instruments) allowing more complex maneuvers in confined anatomical spaces. [GBB+11] [KSHK+21b]
- Improved visualization, often in 3D and high definition, offering better depth perception.
- Tremor filtration and motion scaling, improving fine control in delicate tasks.
- Ergonomic benefits for surgeons (less fatigue, better posture) and possible standardization of surgical quality

1.1 Ureteroscopy (URS) and flexible-Ureteroscopy (fURS)

The formation of kidney stones is a common urological condition that imposes a considerable disease burden globally. In 2021, approximately 106 million cases were reported worldwide [GBD24]. Projections suggest that this condition could affect 25% of the population within 30 years, resulting in reduced quality of life and increased economic costs for healthcare systems and patients. [AAC+25a] [PGS24]. And although, global incidences over the last three decades in most regions show an increasing trend, the fatality rate has stabilized and improved surgical methods have been a contributing factor especially for better surgeon ergonomics and instrument stability [SGT+23].

Ureteroscopy (URS) is a medical procedure for endoscopic inspection/treatment of the ureter (and often renal pelvis) using a rigid or semirigid ureteroscope passed retrograde via the urethra and bladder. Commonly used for ureteral stones, this procedure can also include laser lithotripsy and basket extraction for kidney stones of relatively larger sizes, which cannot be passed naturally through the urinary tract [WL24],[RAP+08].

Flexible ureteroscopy (fURS) is performed with a flexible ureteroscope to access the renal pelvis and calyces for intrarenal stones, and typically followed by the usage of laser lithotripsy, irrigation, and retrieval devices [Cho15], [BOL+08].

The use of fURS continues to grow due to its benefits on the patients recovery. However, it imposes several challenges to the surgeon like unergonomic positions, steep learning pose or lack of spatial awareness due the narrow field of view of the ureteroscope.

Ergonomics and workload represent a major challenge: prolonged fURS requires unergonomic hand and wrist postures, fine deflection control, and continuous visual attention, leading to significant physical and mental fatigue on SURG-TLX and EMG-based evaluations [HHBH+24]. Robotic fURS systems address this issue by transferring instrument control to an ergonomic console, providing tremor suppresion, smoother scope manipulation, and in some cases enabling true solo-surgery. These systems have shown improved ergonomics and usability while maintaining safety and stone-free rates to conventional fURS [SHS+23].

Beyond the ergonomic benefits of robotics, computer vision methods — particularly visual Simultaneous Localization and Mapping (vSLAM) — offer additional support by estimating a 3D map of the kidney and tracking the pose of the flexible ureteroscope's tip within that map. This enhances visualization and navigation, reducing the risk of missed stones [OMSK+23].

Building on this, augmented-reality navigation systems such as NAVIUS [AAC+25b] demonstrate that combining computer-aided 3D maps with the scope tracking and coverage visualizations can enhance the exploration of the kidney and reduce subjective workload.

Additionaly, standard fURS relies heavily on fluoroscopy for orientation, exposing both patient and operating-room staff to ionizing radiation. Navigation systems can reduce fluoroscopy dependence while robotic teleoperation platforms can shift the surgeon away from the radiation field [LJ22], [KJM+22], [YYM+15], [YKT+14b].

Computer-assisted and robotic systems open the door to integrated pressure monitoring, automated safety constraints (e.g., virtual fixtures), smarter fragment-removal strategies, and patient-specific virtual or simulated ureteroscopy for planning and training. Collectively, these technologies target the key pain points of URS—navigation, radiation, ergonomics, and cognitive load—and illustrate how robotic and computer-aided assistance can make stone surgery safer, more efficient, and more scalable as stone burden continues to rise.

1.2 Problem Statement for the Thesis

The thesis aims to provide assistance to address some of the challenges listed above, for the fURS surgery. All the modules of this thesis are tested on a synthetic model of the kidney [ref. fig. 3.4].

Fig. 1.1: Samed GmBH's kindey phantom

Two phases of the surgery are considered here: the *exploration* phase and the *extraction* phase. As the name suggests, the exploration phase is when the surgeon initially explores the renal system, the kidney, its structure, the number and the location of the stones. The methodology assists the exploration phase by allowing the surgeon to have a bird's eye view, which helps in avoiding collisions with the walls of the kidney. The color of the ball changes according to how close is the endoscope from hitting the walls, as shown in fig. 3.25. This is the first visual feedback, i.e. RViz screen.

In endoscopic surgery, the “which way is up?” problem refers to the fact that the endoscopic image has no stable horizon: as the shaft is rotated, the camera view rolls with it, but the monitor does not indicate which side of the image corresponds to the “up” direction of the endoscope or to a fixed anatomical reference. Because of this roll ambiguity, operators sometimes resort to indirect cues to re-establish orientation—for example, spraying a small amount of water or dye through the working channel and watching which way it falls under gravity to identify the dependent side of the lumen. [Sal05]

To address the orientation ambiguity, the methodology introduces an arrow indicator—with a ball representing the endoscope tip on the RViz screen to depict the current direction of the scope. 3.4.2

Fig. 1.2: RViz: the ball represents the endoscope tip, and the color changes according to the distance from the walls of the kidney - *green*: safe distance, *yellow*: borderline-safe distance, *red*: threshold distance, about to collide with the wall

In the extraction phase, the stones with their locations confirmed in the exploration phase, are examined. According to their size, they may need to be fragmented using a laser before extracting the smaller pieces, or, if small enough, they can be removed through the working channel without fragmentation using the basket[AJS+24]. The second visual feedback consists of predefined trajectories guiding the surgeon from the kidney entry point to the different stones, located in the exploration phase. Each trajectory has a safe volume, defining the space in which the ureteroscope should navigate. The surgeon is alerted when the endoscope tip moves out of the safe volume. The safe volume is visually represented by rings, as shown in fig. 1.3. This second visual feedback is given via ImFusion Suite, and will be referred to as ImFusion screen hereafter.

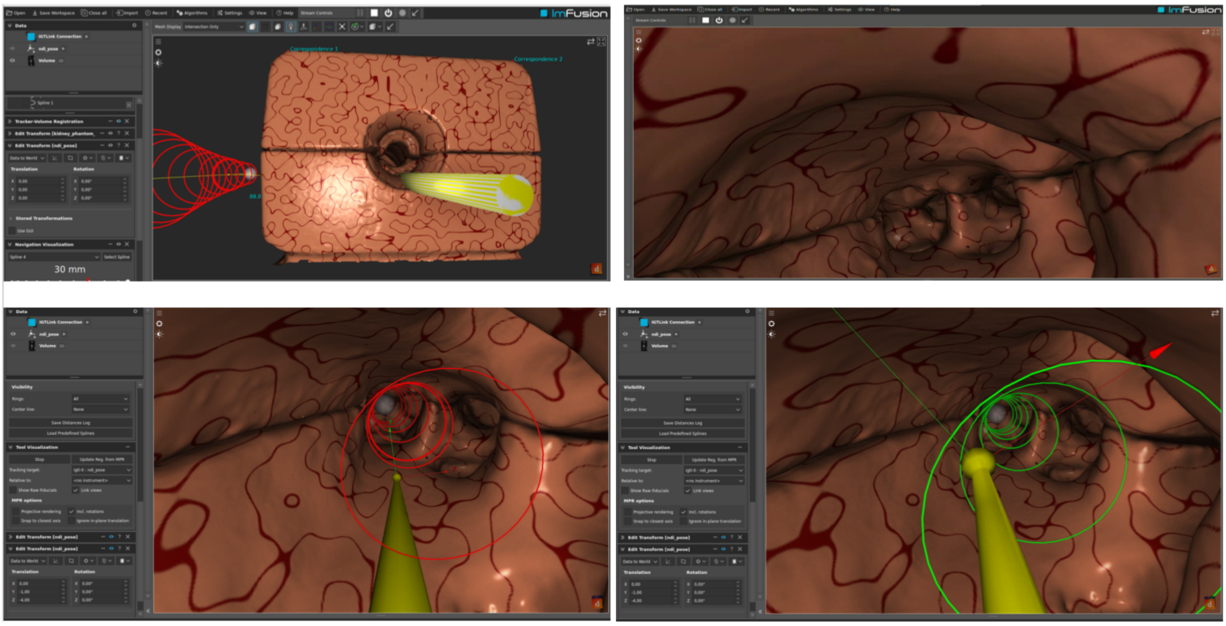

Fig. 1.3: ImFusion Suite: The ImFusion Suite simulates the endoscopic camera view. The view from outside the kidney box (top-left), the view inside the kidney (top-right), the color of the rings shown change according to the deviation from the path - *red rings*: outside safe volume (bottom-left), *green rings*: inside safe volume (bottom-right)

For the collision avoidance in the exploration phase, a threshold distance is set by the user, which signifies the minimum distance between the endoscope tip and the walls of the kidney. Similarly, the radius of the rings for the 'safe volume' in the extraction phase is set by the user, corresponding to the maximum distance a surgeon can deviate from the predefined path.

Besides the visual feedback, there is an additional module for tactile feedback. It is used to alert the surgeons using vibrations on their fingers [as shown in fig. 3.9], according to the threshold distances set in either of the phases.

To evaluate the effects of different feedback modules, and in turn understand the impact of the proposed methodology in this thesis, an exploratory user study was conducted with 13 participants from DLR. All the users completed two sets of tasks in both the exploration phase and the extraction phase. For every task, the participant performed three variants: without feedback, with visual feedback only, and with combined visual & haptic feedback. Out of the two sets, one set intentionally designed to be more demanding. User performance across all conditions was subsequently compiled and analyzed, together with their NASA-TLX responses, to evaluate the improvements attributable to the additional feedback modalities.

Fig. 1.4: FingerTac

2 Fundamentals and State-of-the-Art

2.1 Introduction to the Thesis

Nephrolithiasis (kidney stone disease) refers to the formation of mineral and crystalline aggregates (stones) in the urinary tract, particularly in the kidneys or ureters. These stones arise when urine becomes supersaturated with stone-forming solutes (e.g., calcium, oxalate, uric acid, cystine) and the normal balance of promoters (crystal-forming ions) and inhibitors (citrate, magnesium, pyrophosphate) is disrupted [RAA10], [WZZ+21].

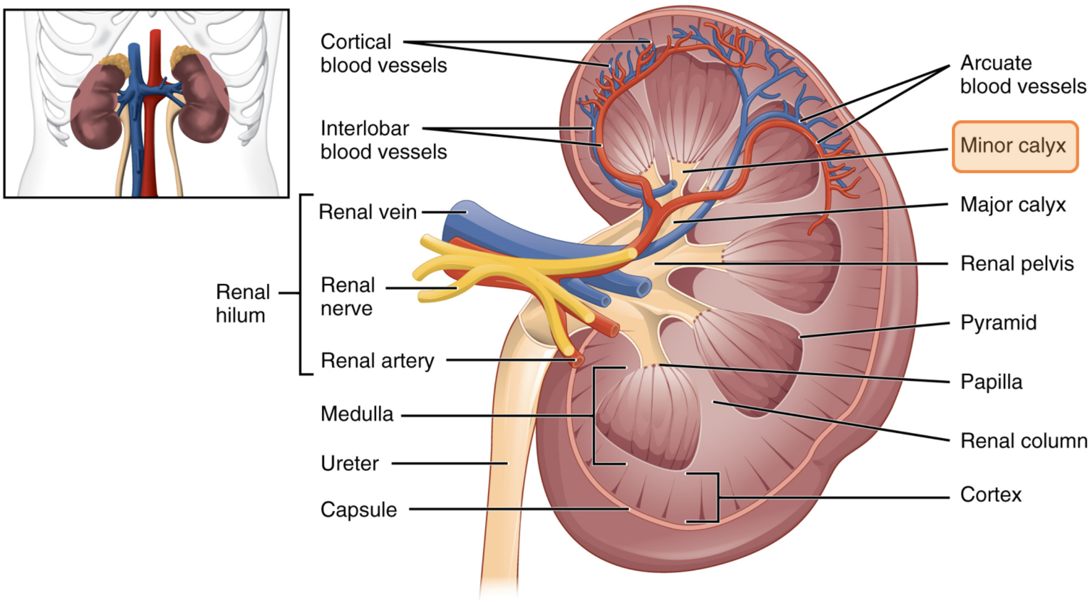

Fig. 2.1: Anatomy of a kidney. The minor calyx is highlighted

The renal collecting system consists of a hierarchical network of chambers that drain urine from the renal papillae into the ureter. Urine produced by nephrons enters the minor calyces, which merge into major calyces, and then into the renal pelvis, which narrows to form the ureteropelvic junction (UPJ). From here, urine flows through the proximal, mid, and distal ureter before entering the bladder at the ureterovesical junction (UVJ). The anatomy of a kidney [Uni25] is shown in fig. 2.1. Here, the minor calyx is highlighted since the methodology presented later operates at the level of individual calyces.

Kidney stone formation arises from a combination of physicochemical, metabolic, and environmental factors that disturb the normal balance of urine composition. Supersaturation of lithogenic solutes promotes crystal nucleation and growth, while reduced levels of natural inhibitors such as citrate or magnesium further facilitate calcium-based stone formation. Low urine volume—often due to inadequate fluid intake or high fluid loss—favors crystal retention, and alterations in urine pH can shift risk toward specific stone types, with acidic urine promoting uric-acid stones and alkaline urine favoring calcium-phosphate stones. Metabolic abnormalities including obesity, insulin resistance, hyperparathyroidism, and various genetic or acquired disorders increase urinary excretion of stone-forming ions. Dietary patterns high in sodium, animal protein, oxalate, fructose, and sugary beverages further exacerbate lithogenic conditions. Environmental and occupational heat exposure, dehydration, and sustained sweat loss also contribute, making stone disease a multifactorial condition strongly influenced by lifestyle and systemic health.

Kidney stones can form or lodge at any part of the renal system, but are most commonly found in the lower-pole calyces, renal pelvis, and natural ureteric constrictions (UPJ, iliac crossing, UVJ).

Because stones can recur (many patients develop another stone within 5-10 years), and because they may lead to complications (pain, obstruction, infection, renal damage), formation of kidney stones is a significant clinical burden.

A growing body of epidemiological research shows that kidney stone disease is increasing globally — both in prevalence and in the burden on healthcare systems. Global studies show more than 115 million incident cases of urolithiasis worldwide in 2019 [ZZP+22]. A recent 2024 study found that disability-adjusted life-years (DALYs) associated with urolithiasis increased in 181 countries between 2000 and 2021 [AHB+24].

Historically, surgical management of kidney stones was dominated by highly invasive open procedures. Early descriptions from ancient civilizations and classical authors such as Celsus and later medieval surgeons focused on perineal lithotomy for bladder stones, with high morbidity and mortality. [TC13]. The modern shift toward minimally invasive, image-guided stone surgery began in the late 20th century with three key developments: extracorporeal shock wave lithotripsy (ESWL) in the early 1980s; percutaneous nephrolithotomy (PCNL), first reported in 1976 by Fernström and Johansson and later refined as the standard for large and complex renal stones; and ureteroscopy (URS), which evolved from early rigid instruments to modern flexible ureteroscopes that can access virtually all calyces under fluoroscopic and endoscopic guidance [BNV+19], [MHP+20]. These advances progressively reduced incision size, blood loss, length of stay, and complication rates compared with traditional open stone surgery, which now has only a limited role for very complex or salvage cases [HDC+24].

Over the last few decades, flexible ureteroscopy (fURS) and retrograde intrarenal surgery (RIRS) have become central to the management of small–moderate renal stones, benefiting from improvements in optics, deflection, laser lithotripsy, and ureteral access sheaths [AAEN+19], [BS17]. In parallel, advanced imaging and navigation have made these procedures increasingly image-guided, with real-time fluoroscopy, 3D CT reconstructions, and, more recently, augmented-reality navigation systems that provide scope localization and coverage maps of the collecting system [HDC+24]. At the same time, epidemiological studies show that the incidence and prevalence of kidney stones are rising globally, across sexes, age groups, and regions, driven by changes in diet, obesity, metabolic syndrome, and environmental factors. This rising stone burden — larger stones, more stones per patient, and higher recurrence, places increasing demands on endourologic procedures such as fURS: instruments must navigate more complex collecting systems, fragment removal must be more efficient to avoid residual fragments, and operative times and surgeon workload are pushed higher [ÇAT+25], [Wis22].

Moreover, the typical stone patient now more often presents with metabolic and systemic comorbidities—including obesity, diabetes, chronic kidney disease, and prior interventions—which can alter renal function, anatomy, and perioperative risk. These trends underscore that modern stone surgery cannot rely on endoscopic visualization alone: there is a growing need for assistive systems (e.g., navigation overlays, pressure monitoring, enhanced fragment evacuation tools), optimized workflows (instrument pathways, access sheath strategies, staged procedures), and integrated preventive strategies (metabolic evaluation, dietary counseling, and long-term surveillance) to maintain high stone-free rates while managing surgeon workload and patient risk. In this context, the historical journey from open surgery to MIS and image-guided fURS is still ongoing, with the next phase focused on smarter, more supportive platforms which can assist the surgeons better and result in quicker recovery times for the patients.

2.2 Assistive modules in fURS

Current ureteroscopes have a limited field of view, requiring significant experience to adequately navigate the renal collecting system. This is evidenced by the fact that inexperienced surgeons have higher rates of missed stones. One-third of patients with residual stones require re-operation within 20 months [AAC+25a].
The limited field of view during the surgery poses significant challenges for urologists by negatively impacting navigation and kidney stone treatment [KO22].
Robotically assisted systems have increasingly been proposed to overcome the intrinsic perceptual and ergonomic limitations of conventional minimally invasive surgery. As reviewed by Klodmann et al. [[KSHK+21a]], modern RAS platforms aim to enhance surgeon perception, dexterity, and situational awareness through advanced sensing, imaging, and control architectures.

The main challenges and how integration of computer or robotic assistance can ease them, are mentioned below:

- **3D perception**: Since the endoscopes have monocular cameras, it makes it harder for 3D perception [as shown in 2.2], especially in narrow calyces, resulting in constricted navigation and impacts the decision making.
  A 3D view might help in the understanding the 3D structures inside the patient.

- **Spatial localization inside the collecting system:** During the procedure, a flexible ureteroscope must be maneuvered through a complex 3D environment [TMW+17a], for example which calyx is being currently analyzed, how far is the surgeon from a landmark, or a stone and at what angle is the endoscope. In fURS

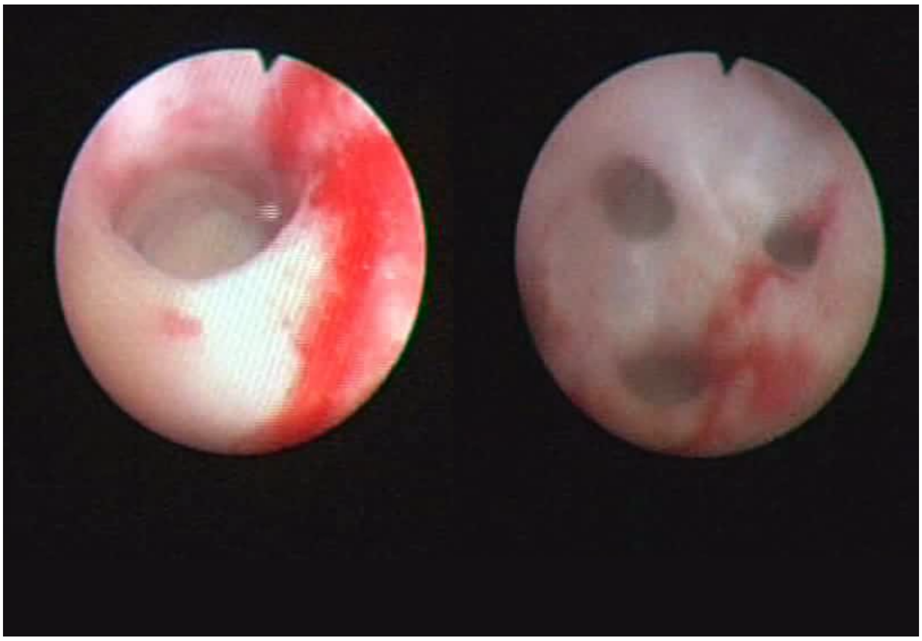

Fig. 2.2: The only available visual aid for surgeons: screenshots of the monocular camera's view from live surgery; It shows two different instances of the surgery from the same endoscopic feed

surgeries, the urologist is not always sure of the positioning of the ureteroscope tip in the anatomy.
Real-time motion tracking registered to pre-operative data or a SLAM system synchronized with endoscopic video provide a bird's-eye view of the ureteroscope's position inside of the kidney.

- **Ergonomic limitations**: For surgeons or the personnel operating the uroteroscope, prolonged constrained hand/wrist postures and foot controls have been associated with an increased risk of work-related musculoskeletal injury [HPC+11].
Systems like remote consoles, telemanipulators, and solo surgeries using a robotic arm help in mitigating this.

In recent years, visual guidance in minimally invasive surgery has advanced from traditional 2D endoscopic views to navigation-grade augmented overlays. In urological procedures in particular, visual feedback systems have been developed to register preoperative imaging data, such as CT scans, with the renal collecting system, enabling real-time ureteroscope-tip localization, visualization of explored areas coverage, and stone annotation. These innovations have demonstrated improved procedural coverage and reduced operator workload in phantom studies.

Haptic feedback is re-emerging with better sensors and wearables. Systematic reviews across robotic MIS report consistent performance gains in speed and accuracy, resulting in lower errors and workload, from haptics or vibrotactile cues. The field has shifted from heavy kinesthetic arms to lightweight, wearable, or local endoscopic sensing [Ber23] [SDA24].

In fURS, demand for navigation assistance continues to grow, with platforms adding 3D tip tracking and AR image overlays [TMW+17b], [RSHK+22], [AAC+25b] alongside emerging intra-renal pressure monitoring to enhance safety, [LJ25], [SDE+25], [BMB+25], [PBCV24], [BCS+24], [YCY+25] recent robotic systems emphasize safety features such as virtual fixtures while preserving native haptics through manual actuation [SHS+23], [LDMFD24], [SHW+22], [RSHK+22], aiming to improve clinical outcomes, shorten hospital stays, and enhance ergonomics and surgeon independence via efficient solo-surgery workflows [GIS+25].

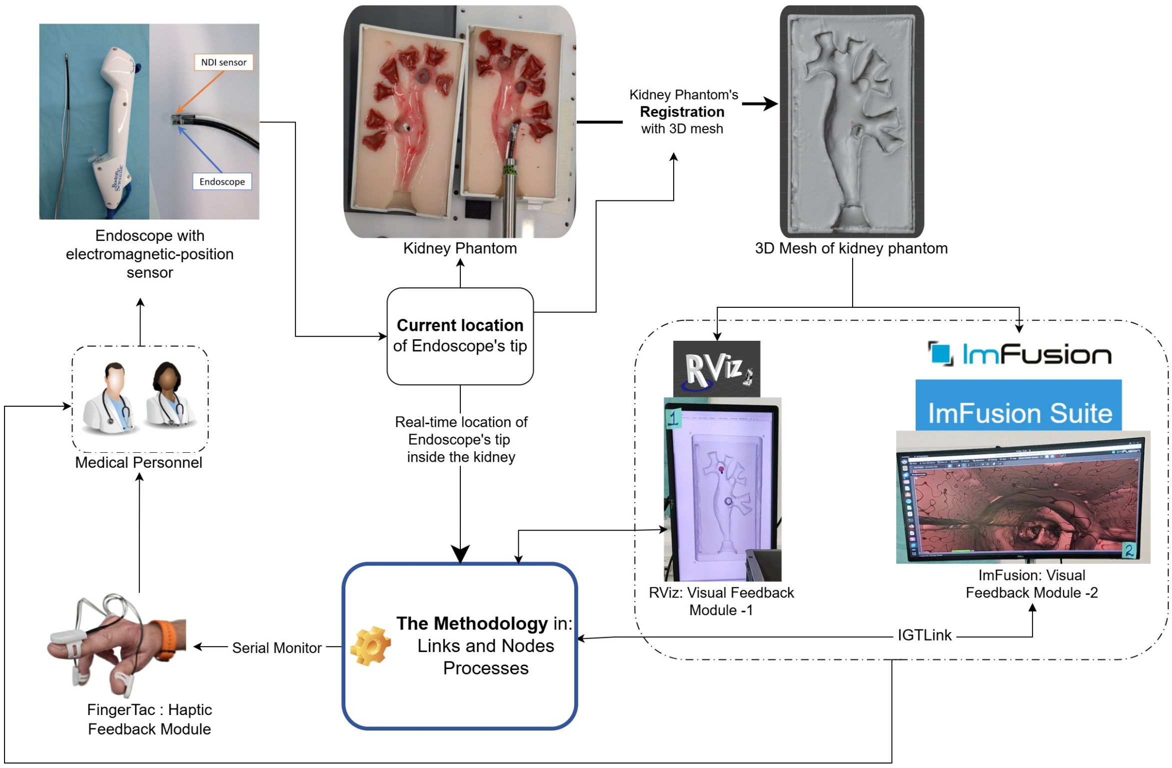

Fig. 2.3: Basic Outline of the Modules in this Thesis

In the next section, this thesis will be explored in detail: the setup including the hardware, the software, their integration and the methodology used. The methodology provides a bird's eye view of the renal collecting system by visualizing the 3D structure of the kidney together with the real-time tracking of the endoscope tip during the surgery. Two types of feedback modalities will be present: visual and haptic, which are used to assist and alert the operator with the endoscope. The threshold parameters for triggering the alerts can be fine tuned by the user. A basic outline is shown in fig. 2.3.

The system presented here primarily covers the two phases of the fURS surgery: the exploration phase (or the collision-avoidance phase), and the extraction phase (or the guidance phase).

Exploration phase corresponds to the basic exploration of the kidney at the start of the surgery, to assess the anatomy, and identify the location, size, number, and composition of stones. This phase also helps surgeons plan the stone treatment/extraction strategy based on the outcome of the exploration and other parameters related to the patient. In this phase, the system presented will help explore the renal system, alerting the surgeons when the endoscope tip is about to collide with the walls of the kidney, while giving a bird's eye view of the renal system with live tracking of the endoscope tip. This will help the surgeon with spatial localization and quicker and safer navigation inside the kidney.

In the extraction phase, stones may be removed directly with a basket or fragmented using a laser, after which the smaller fragments are either retrieved with the basket (examples shown in fig. 2.4 [Coe]) or allowed to pass naturally if they are small enough. In this phase, surgeons will be suggested pre-planned paths from the entry point of the kidney to the location(s) of the stone(s). Visual cues will change when the surgeon moves inside or outside the safe volume of the pre-planned path.

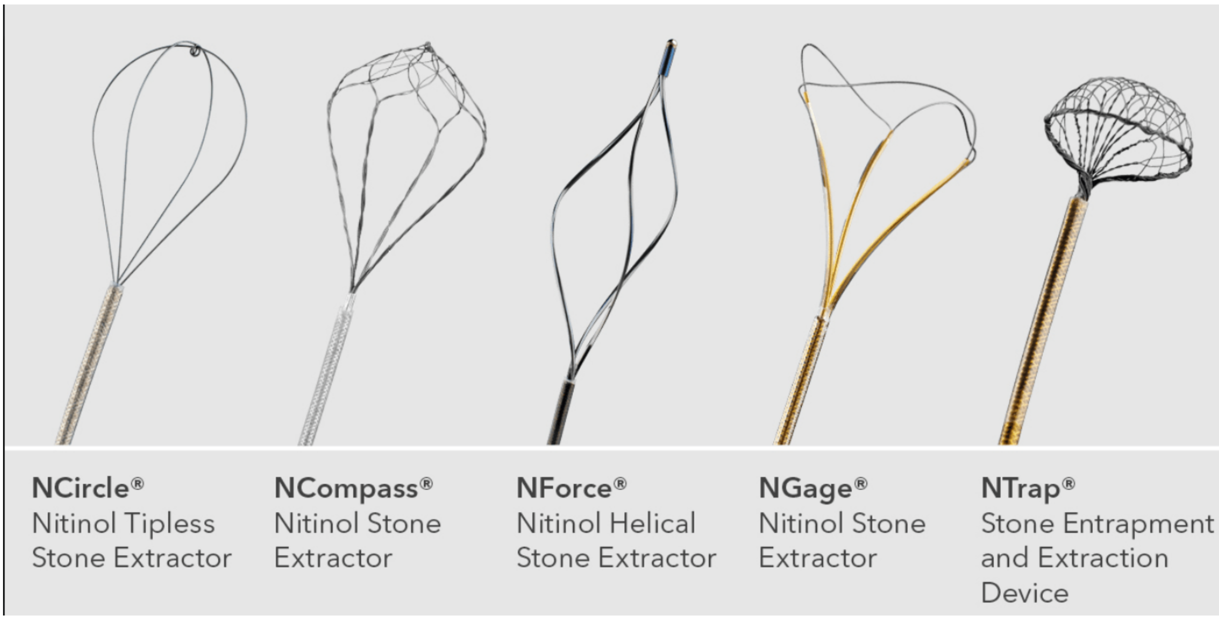

Fig. 2.4: Examples of 'basket' tools used for the extraction of kidney stones

The haptic feedback here is given via vibrations on the fingers of the operator, which are a part of alerting the surgeons when they are about to collide with the walls of the kidney or when the deviations from the pre-planned trajectories are too high.

All the feedback cues can be individually stopped and restarted by the person operating the desktop system on which the feedback modules are running.

After a quick introduction in section 3.1, the hardware and the software used will be explAINED in sections 3.2 and 3.3 respectively. This methodology under section 3.4 will cover all the components, including the parts for visual and haptic feedback modalities, their initialization and setup, and the integration.

Section 3.6 will have the details of the feedback modules for the exploration phase, and section 3.7 will cover the extraction phase and the related feedback mechanisms. The exploratory study, its corresponding results, and the interpretations derived from them will be presented in Section 4. Section 5 will outline potential extensions of this work that were beyond the original scope of the thesis. The overall concluding remarks of the thesis will be presented in section 6.

A few systems incorporating visual and haptic assistance are currently being developed and evaluated across various surgical domains. These systems integrate functionalities such as visual navigation, scope-tip tracking, haptic feedback, and augmented reality. The first clinical implementation of a master–slave robotic platform for flexible ureteroscopy (fURS), the Sensei-Magellan system, was introduced by Desai et al. in 2008 [AD09]. Additional state-of-the-art systems are briefly discussed below.

2.3 Current State-of-the-Art Systems

- **'Novel ureteroscopic navigation system with a magnetic tracking device:'** This system helps with Visual navigation via an UI with anatomical map and trajectory cues. It uses a magnetic tracker on the ureteroscope for accurate orientation of the tip of the ureteroscope [YKT+14a].
  This positional data is processed to update a graphical display that assists the surgeon in navigating the renal collecting system with improved precision and reduced reliance on fluoroscopy.
  The workflow integrates with standard ureteroscopic procedures, requiring minimal modification to existing setups. However, the system's performance is limited by magnetic field distortion in metallic environments, potential calibration drift over time, and the absence of force or tactile feedback to complement visual cues.

- **'An ORB-SLAM3-based approach for surgical navigation in ureteroscopy':** Oliva-Maza et al. [OMSK+23] extend ORB-SLAM3 [CER+21] to accurately estimate the sparse 3D map of the kidney and the position of the ureteroscope's tip using only the ureteroscope images without the need of extra sensors.
  The sparse 3D map together with the position of the ureteroscope are shown in the ORB-SLAM3 GUI, helping the surgeon navigate inside the kidney. However, surgeons must still manually explore the entire kidney to ensure that no stones remain. A limitation here is the assumption of a static environment, which degrades performance when tools move or the kidney stones were already extracted.

  A few state-of-the-art systems illustrate how visual cues are being integrated into endoscopic navigation:

- **'NAVIUS: Navigated Augmented Reality Visualization for Ureteroscopic Surgery':**
  The NAVIUS model aims to enhance spatial awareness during flexible ureteroscopy by providing real-time visual navigation through an intuitive user interface that displays an anatomical roadmap and trajectory cues. The system employs a small magnetic sensor affixed near the tip of the ureteroscope, allowing continuous tracking of the instrument's three-dimensional orientation and position within a pre-acquired anatomical model [AAC+25a].
  It integrates pre-operative CT or MRI–derived 3D reconstructions of the renal collecting system with intra-operative electromagnetic (em) tracking of the flexible ureteroscope to provide augmented-reality (AR) guidance through a HoloLens 2 display.
  This workflow eleviates spatial orientation and situational awareness during flexible ureteroscopy. However, potential EM-field distortions near metallic instruments, the absence of haptic feedback, the added hardware complexity, and the cognitive demands of head-mounted AR visualization constrain immediate clinical translation

- **TIMS: A Tactile Internet-Based Micromanipulation System with Haptic Guidance for Surgical Training:**
  This is a Tactile-Internet microsurgical training platform that combines web-based teleoperation with haptic guidance to help trainees reproduce expert motions during micromanipulation [LGF+23].
  It restores the sense of touch, reducing cognitive load—surgeons don't need to constantly toggle views or overly rely on visuals to gauge tool-tissue proximity

- **'da Vinci Surgical System (Intuitive Surgical)':**
  The da Vinci platform is a master–slave robotic system for minimally invasive surgery that provides the surgeon with highly magnified 3D HD vision from an endoscopic camera, combined with motion scaling and tremor filtration for precise tool control. An integrated vision stack, including Firefly® near-infrared fluorescence imaging, offers real-time visualization of vessels, perfusion, and biliary anatomy, making the procedure essentially fully vision-driven in the absence of native haptic feedback [DMS+21], [Int25], [Int23].

- **Wrist-Squeezing Force Feedback Improves Accuracy and Speed in Robotic Surgery Training by MPI** [MCC+22]
  The system provides tactile, haptic feedback via wrist-squeezing actuators worn on both wrists. These are servo motors in 3D-printed frames attached to the user's wrists via hook-and-loop straps
  This wearable, lightweight system offers differential feedback on each wrist corresponding to the specific instrument in use, thereby enhancing speed, accuracy, and learning outcomes in robotic surgery training
  The study conducted shows higher accuracy without sacrificing speed, i.e., improved learning on the speed–accuracy frontier. Independent work likewise reports that adding instrument-vibration haptics to robotic simulation reduces perceived workload in both sim and live OR contexts, reinforcing the value of haptic cues for training

and performance.

3 The Setup, Integration and Methodology

3.1 Introduction

The multimodal feedback algorithm presented in this thesis gives additional inputs to the person operating the endoscope, via two visual and one tactile feedback module.

For the visual modules, a 3D mesh of the kidney phantom was generated using a laser scan. The first visual module, using Rviz visualization, gives a bird's eye view of the kidney, the current real-time location of the endoscope tip, and an arrow indicating the direction in which the endoscope will bend – to give the orientation of the endoscope, as shown in Fig. 3.1. The second visual module, using ImFusion Suite, shows additional guiding rings for navigation, simulated kidney stones, and simulated endoscopic camera view of the kidney – replicating the current default conditions for surgeons without any additional feedback, as shown in Fig. 3.26.

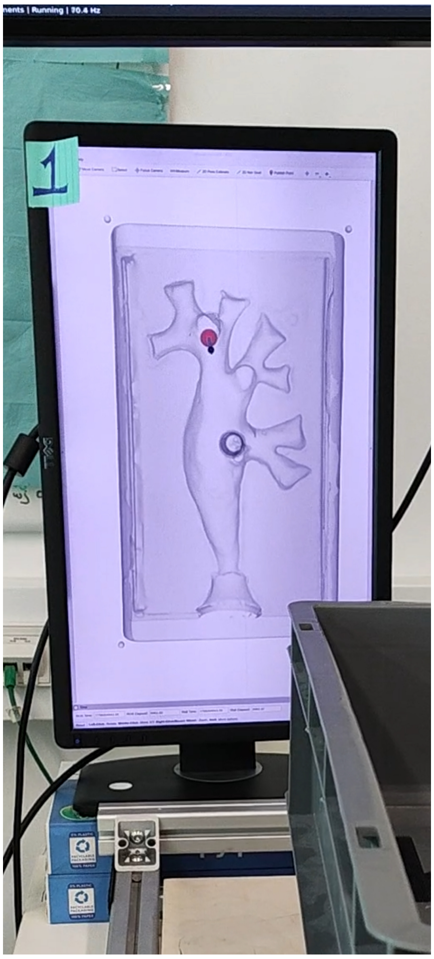

Fig. 3.1: 1st Visual Feedback Module: RViz screen

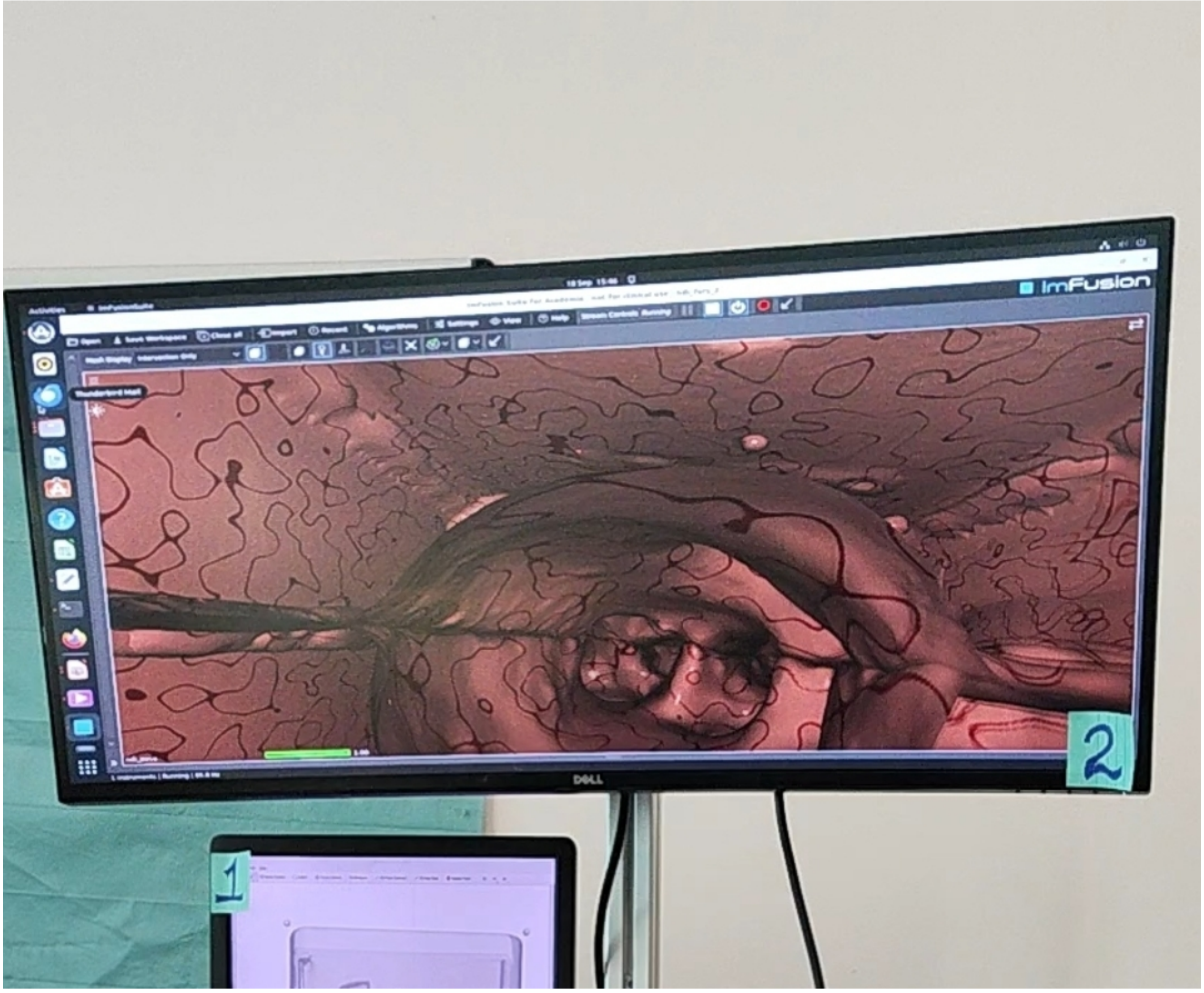

Fig. 3.2: 2nd Visual Feedback Module: ImFusion Suite Graphical User Interface (GUI)

For the tactile module, FingerTac – a wearable haptic device on the fingers, developed in-house in DLR, is used for alerting the users with two different vibration patterns. The FingerTac is attached to the user's hands as shown in fig. 4.5.

The modules function according to the endoscope tip's current position relative to the kidney. Communication among all modules, including the endoscope tracking and kidney registration modules, is handled through Links and Nodes. Links and Nodes is a process management and real-time capable communication middleware for distributed systems.

3.2 Hardware:

1. **kindey phantom**: Samed GmBH's kindey phantom modules were used as shown in [3.4]

2. **Endoscope**: LithoVue^{TM} Single-Use Digital Flexible Ureteroscope from

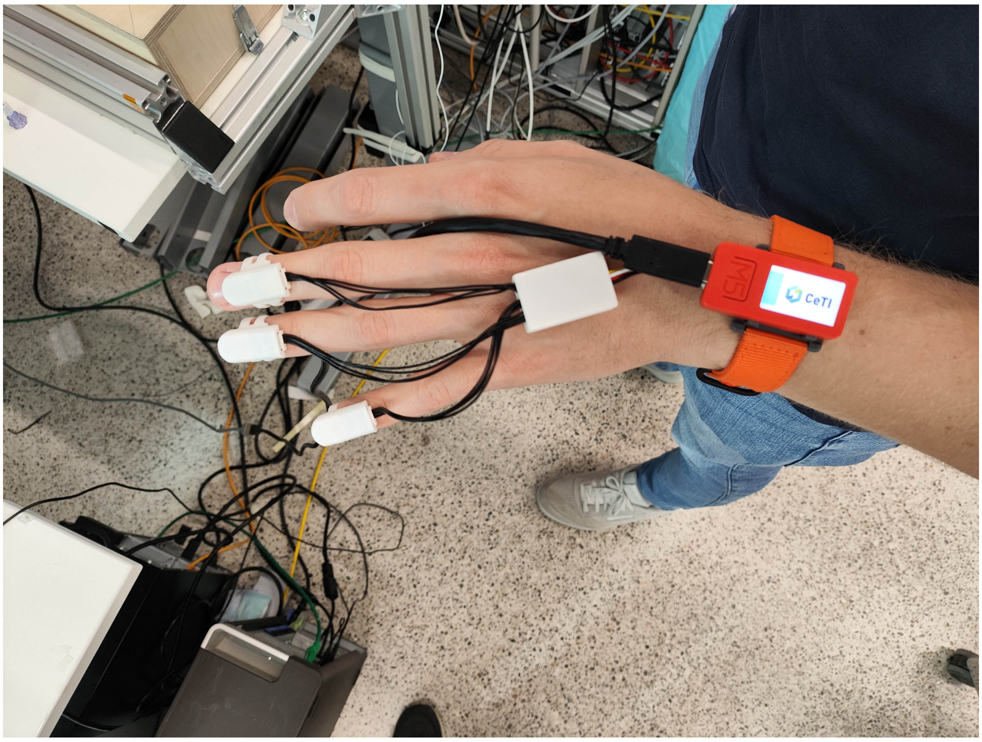

Fig. 3.3: An user wearing the FingerTac

Fig. 3.4: Samed GmBH's kidney phantom

Boston Scientific was used for entering the kindey phantom as shown in [Fig. 3.5]. The endoscope has a flexible tip which can bend in two directions as shown in Fig. 3.6.

Fig. 3.5: LithoVue^{TM} Single-Use Digital Flexible Ureteroscope from Boston Scientific

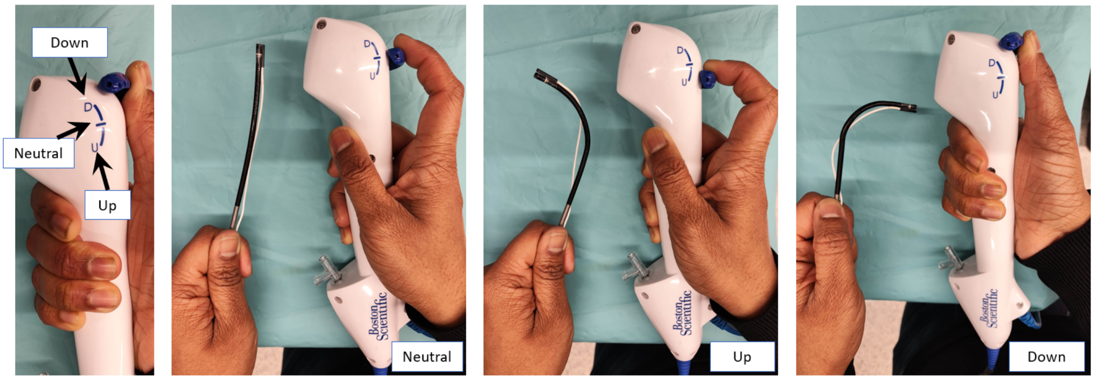

Fig. 3.6: Bending in the Endoscope

3. **Electromagnetic position sensor** – NDI Aurora system:
   The Aurora and 3D Guidance electromagnetic (EM) tracking solutions by NDI, work by generating a defined EM field in which EM micro-sensors are tracked.
   It has 4 main components: the Field Generator (FG), the System Control Unit (SCU), the Sensor Interface Unit (SIU), and the Sensors.
   Principle: A field generator (FG) creates time-varying magnetic fields in a known 3D volume, referred to as the 'measurement volume' from here on. Tiny wire-wound sensor coils embedded in an instrument experience changing magnetic flux and produce voltages. By demodulating these voltages and comparing them to a pre-characterized field map, the system solves for the sensor's 6-DoF/5-DoF pose. The 6-DoF sensor was used, acting as a localization point within the measurement volume, with position and orientation data relayed to the host interface for visualization.

In this thesis we use a 6DoF em-sensor with a position accuracy error of 0.8mm and a orientation accuracy error of 0.7º.

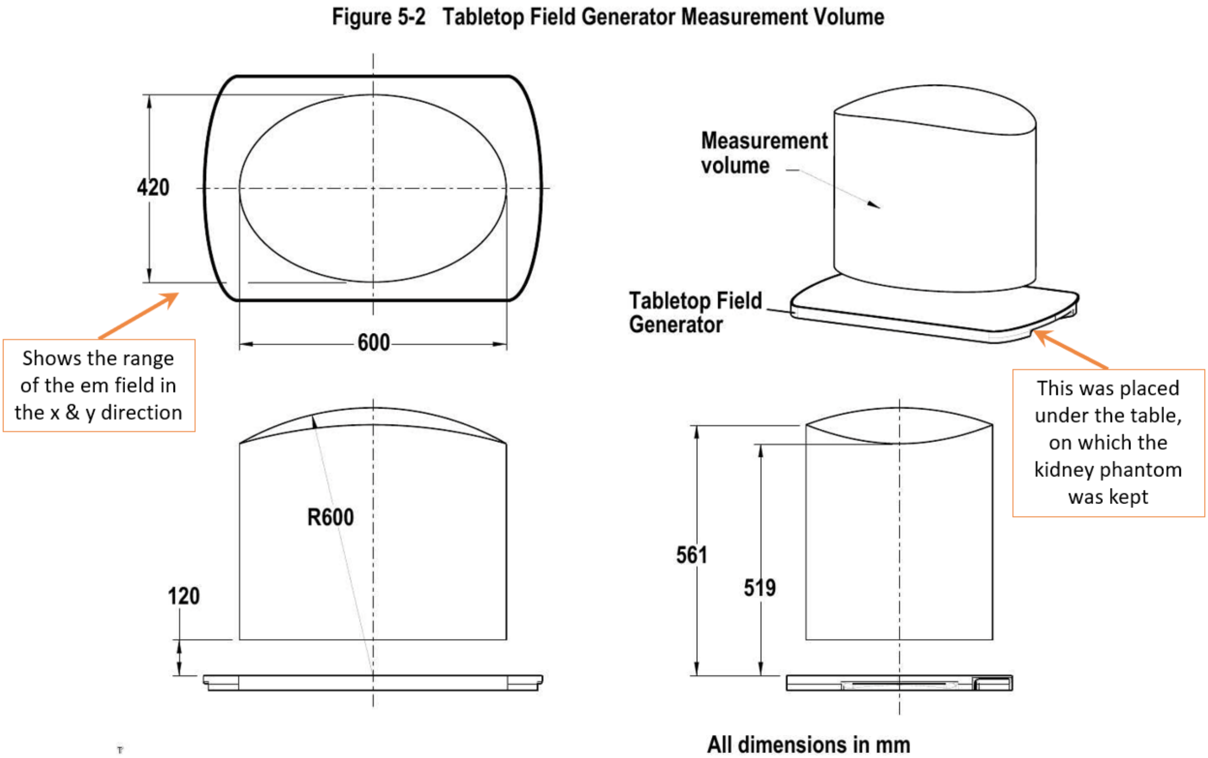

Fig. 3.7: Diagram showing the measurement volume for NDI Aurora em generator.

Working setup: The kidney phantom and the endoscope with the NDI em position sensor were located inside the measurement volume (as shown in fig. 3.7). The em position sensor was connected via a wire to a DLR desktop system. The sensor was placed next to the endoscope's tip as shown in Fig. 3.8, which relayed the position and the rotation data to the DLR system, which could be accessed via Links and Nodes.

4. **FingerTac**: It is a wearable haptic device [Fig. 3.9], developed by DLR using M5StickC PLUS ESP32 Mini IoT Development module, that combines virtual tactile feedback at the finger with real-world interactions

3.3 Frameworks and Software:

1. **Blender**: It is a free, open-source, community-driven 3D computer graphics software, which was used to refine the laser-scanned mesh of the kindey phantom and calculate geometrical points on the mesh [Ble].

2. **Meshlab**: is also a 3D computer graphic software, which was used to fix the geometry of the 3D mesh and decrease the mesh size, so that computation and visualization

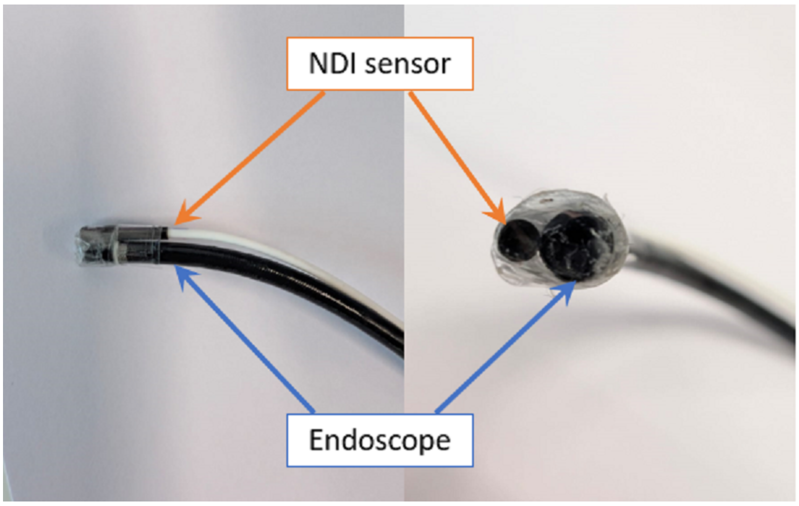

Fig. 3.8: NDI position sensor stuck to Endoscope's tip

Fig. 3.9: FingerTac

becomes faster [Mes].

3. **ROS (Robot Operating System)**: ROS [ROS25] is an open-source robotics middleware and toolset that provides libraries and tools to help software developers create robot applications. It provides hardware abstraction, device drivers, libraries, visualizers, message-passing, package management, and more.

4. **RViz (ROS-Visualization)**: RViz [RVi] is the standard 3D visualization GUI for ROS. It helps visualize robot models (URDF), TF frames, point clouds, maps, trajectories, markers, and camera streams, and interact with planning plugins.

5. **ImFusion GUI**: ImFusion [ImF] Suite is a medical-imaging GUI built atop the ImFusion SDK for rapid prototyping and deployment of advanced image processing and visualization

6. **Arduino Integrated Development Environment (IDE)**: The Arduino Integrated Development Environment is the official desktop app for writing, compiling, and

uploading Arduino "sketches" (.ino) to boards [Ard].

7. **Links and Nodes**: A process management and real-time capable communication middleware for distributed systems developed and used in DLR.

3.4 Methodology

3.4.1 Phantoms and Simulations:

For making the prototype of the methodology, following components were used:

1. The real kidney was modelled by kidney phantom model

2. The 3D reconstruction of a patient's kidney from their CT scans, or the estimated 3D map of the it using SLAM, was replaced by the laser-scanned mesh of the kidney phatom

3. The live feed from the endoscope's camera was replaced with a simulation in the ImFusion Suite

3.4.2 Setting up the components for Visual Feedback

- **3D Mesh of the Kidney Phantom:**

  1. The three parts of the kidney phantom were scanned using a laser scanner obtaining 3 poinclouds that where later converted to meshes - the top view of the kidney phantom box from outside, and the inside areas (when the kidney phantom box is split open, as shown in fig. 3.10).

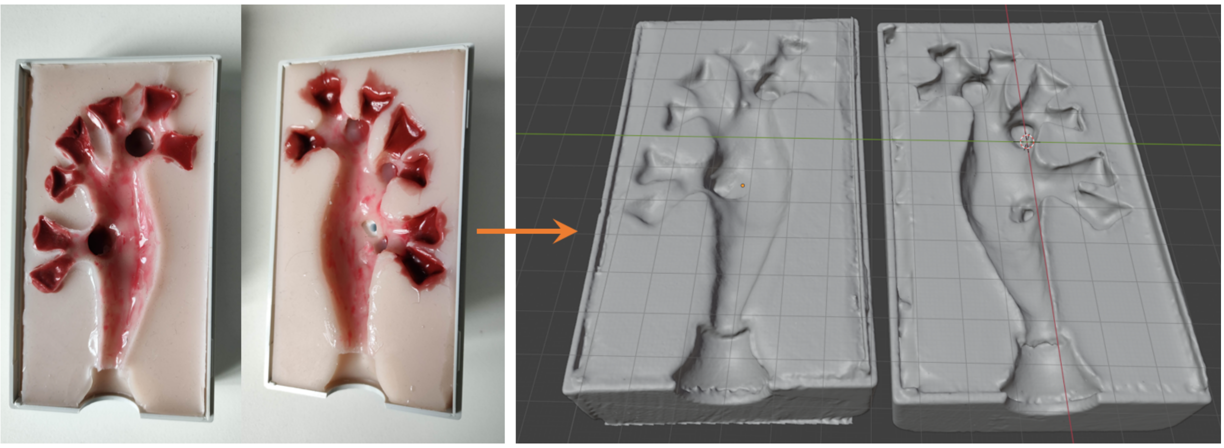

Fig. 3.10: The scans of the insides of the kidney phantom

2. All the individual parts were de-noised using Meshlab and Blender, as shown in fig. 3.11

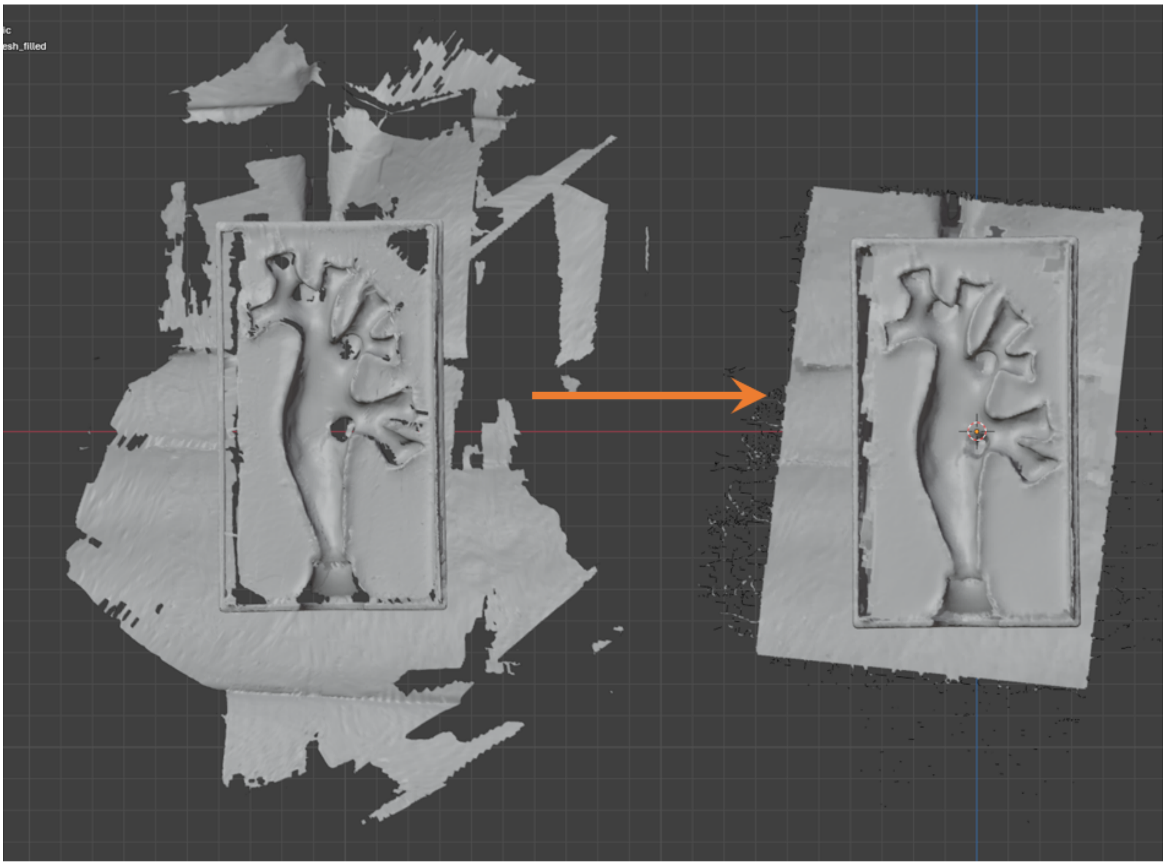

Fig. 3.11: De-noising and closing the holes of the initial mesh

3. The holes in the 3D mesh were cleaned using the python package open3d, with very high number of points to fill the holes, since the kidney mesh was complex and very irregular. The final mesh used was as shown in Fig. 3.12

4. Duplicate vertices and extra faces were removed using Meshlab to bring down the size of the mesh. This helped in faster computation and loading of the mesh for visualization

5. The three individual cleaned parts were finally aligned, as hown in fig. 3.13

- **Registration of the 3D mesh in Rviz/ImFusion Suite with the kidney phantom:**
  Since the kidney phantom box was scanned with a laser to generate a 3D version, the resulting 3D mesh needs to be registered with the kidney

Fig. 3.12: The de-noised mesh, after filling up of irregular holes

phantom, 4 corner points of the box for registration were chosen.

Due to the curved shape of the kidney phantom box, as shown in Fig. 3.14, we had to estimate the corner points of the top surface of the mesh and the kidney phantom box. To get the corner points of the kidney phantom, the next steps were followed (Fig. 3.15):

1. A few points were scanned on one surface of the kidney phantom, using the em-position sensor, as shown in Fig. 3.16. The coordinates of the points were saved

2. Once the points of a surface of the kidney phantom box were saved, a best-fit plane for those coordinates, was calculated using the skspatial package by Python

3. Now, one plane, corresponding to one surface of the kidney phantom box was calculated and the plane's centroid and normal were stored

4. Two adjacent planes, corresponding to adjacent surfaces were calcu-

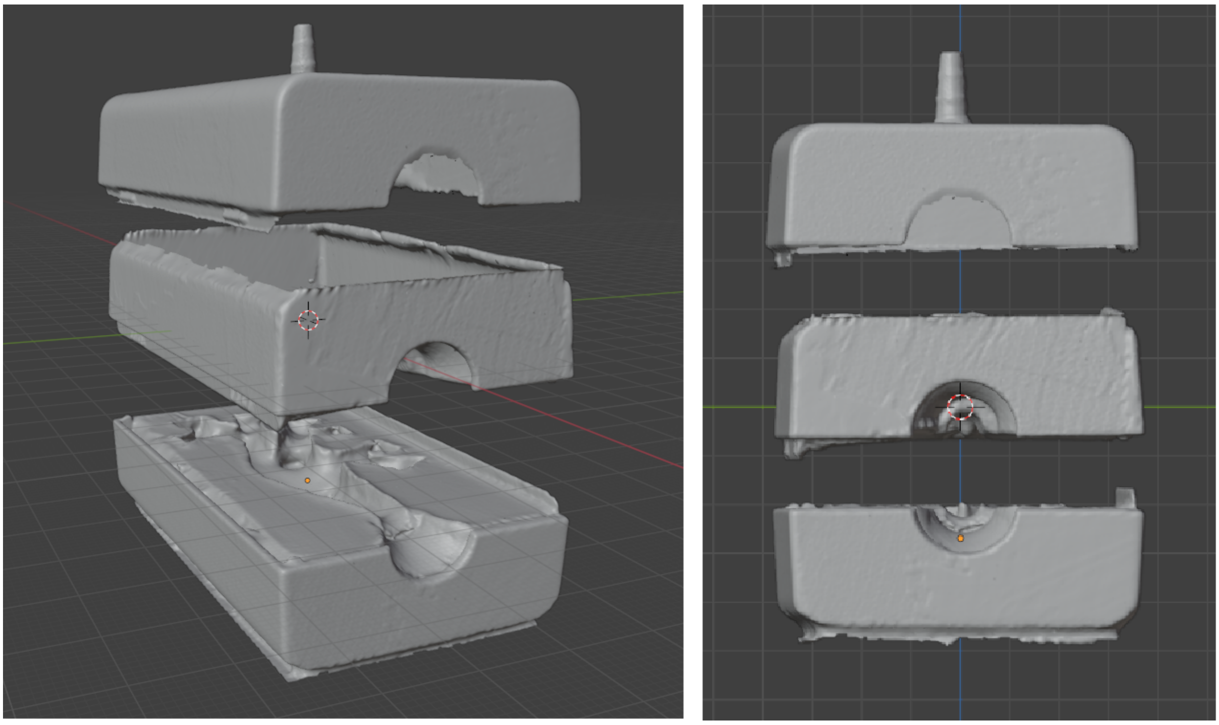

Fig. 3.13: Alignment of the three cleaned, de-noised and filled parts

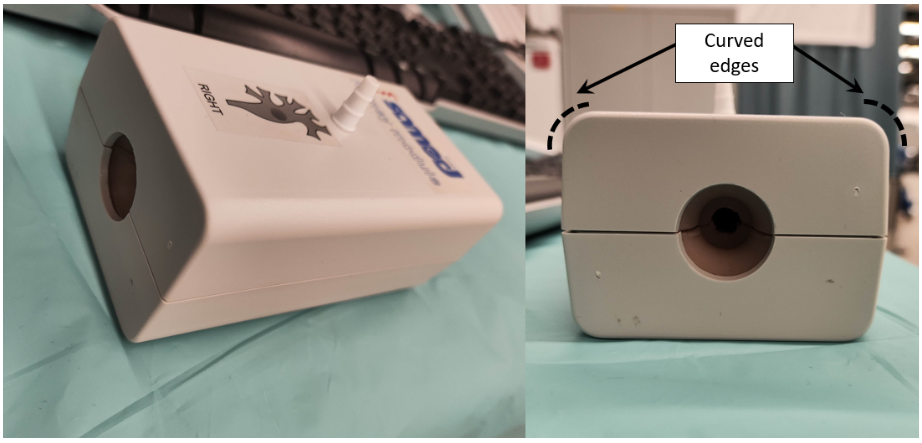

Fig. 3.14: Curved edges of the kidney phantom box

lated in a similar manner

5. Hence, now three adjacent planes (as shown in the example Fig. Fig. 3.17) were calculated and stored

6. The intersection of the 3 planes in the above step was calculated and stored as the corresponding corner point

7. The 4 corner points, as pointed with the kidney phantom model

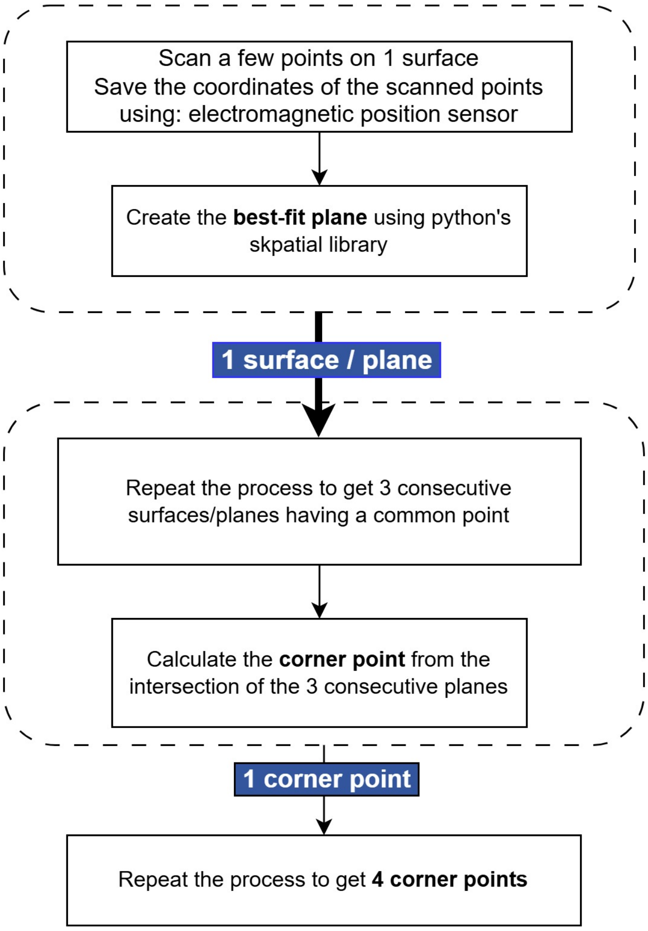

Fig. 3.15: Workflow to get the corner points of the kidney phantom box

Fig. 3.21 were calculated in the same manner (steps 1 → 6). The corner points were stored in a specific sequence as shown in Fig. 3.18, and the x,y,z coordinates of these 4 corner points were saved

8. For the 3D kidney mesh, Blender's scripting feature was used to select points on 3 consecutive surfaces and then calculate the corresponding best-fit planes using the principal component analysis (PCA) method. The intersection of those 3 planes were calculated and stored as a corner point, as shown in Fig. 3.19 and Fig. 3.20.

9. The above step was repeated 4 times to get 4 corner points in Blender, as shown in Fig. 3.21

10. The 4 corner points and the mesh were saved as a single file in Blender. The next task was to separate this single blender file into 5 sub-meshes

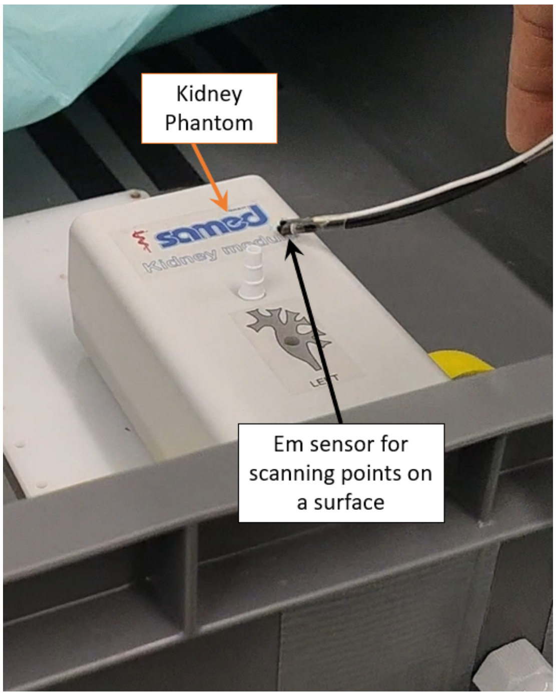

Fig. 3.16: Using em position sensor to scan and save some points on a surface. The coordinates of those points, as sent by the position sensor were saved

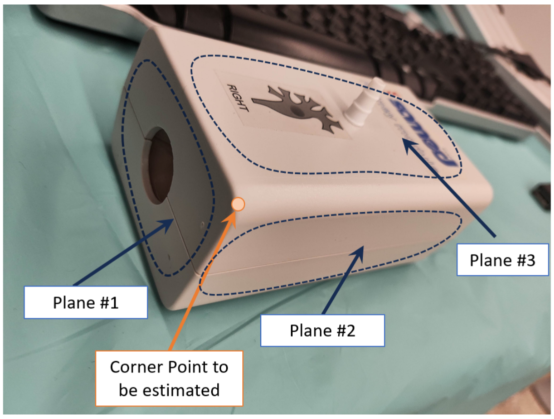

Fig. 3.17: 3 adjacent surfaces of the kidney phantom box, and the corresponding corner point from their intersection

(4 corner points + 1 kidney mesh).

11. Getting the corner points from the 3D mesh file in Blender: the python package 'trimesh' was used to separate the single meshes into 5 separate sub-meshes: 1 main mesh + 4 corner points. The coordinates of the 4 corner points were sorted according to their x,y,z values, as shown in Fig. 3.21, to match the sequence of the corner points of the real kidney phantom (ref: Fig. 3.18).

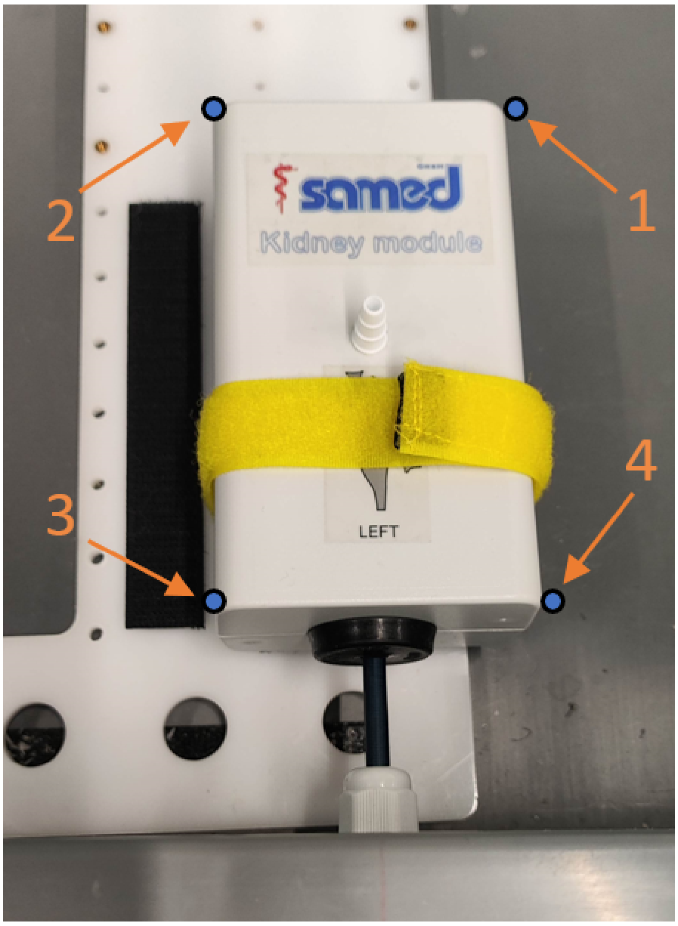

Fig. 3.18: These 4 corner points were calculated and used for registration with the 3D mesh

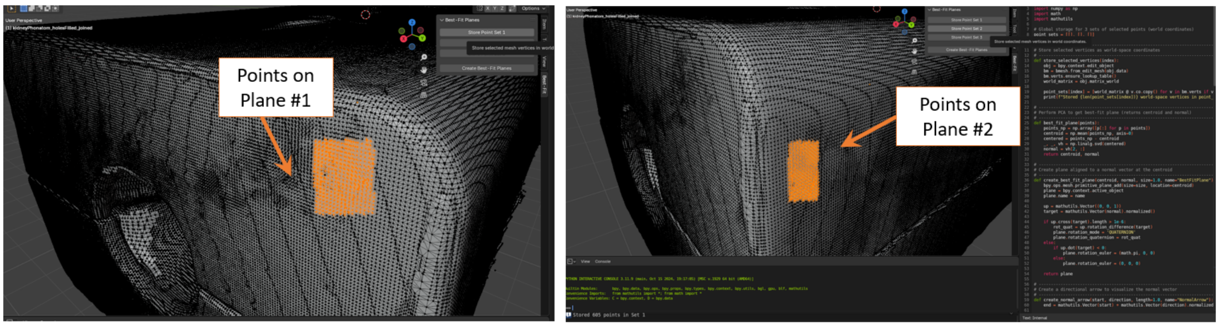

Fig. 3.19: Selecting points on a plane in Blender

12. Now, we had 4 sorted corner points for the 3D mesh, and 4 corner points for the kindey phantom box in the same sequence

13. For transformation of the 3D mesh (in python coordinate system) to the kindey phantom box's location (in NDI's coordinate system): A script was run to calculate a transformation matrix, given 2 sets of 4

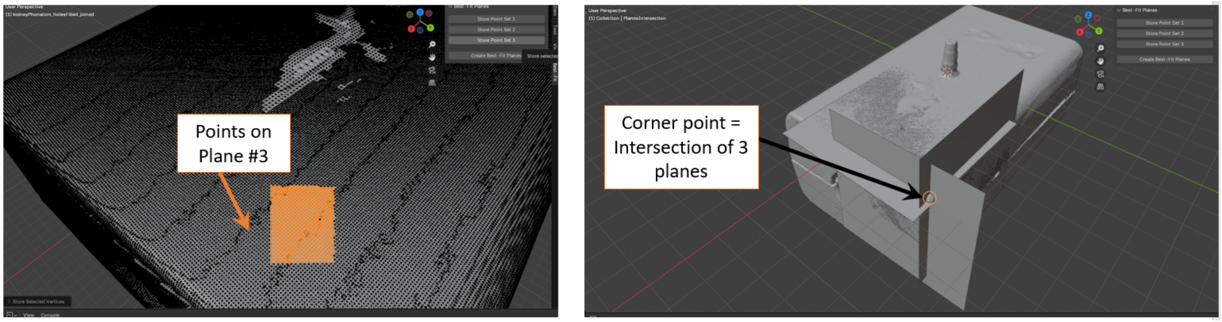

Fig. 3.20: Selecting points on a plane in Blender and calculating the intersection of the 3 planes to get a corner point

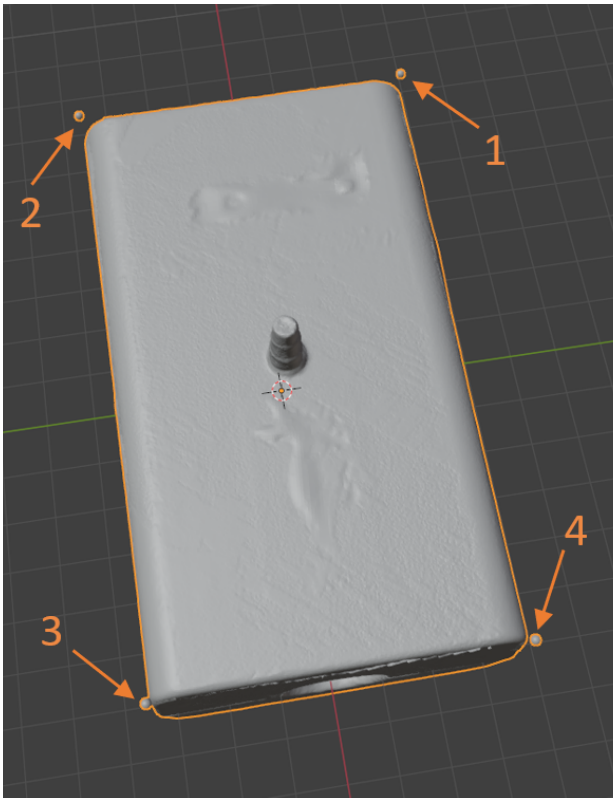

Fig. 3.21: 4 virtual corners of the top surface of the 3D mesh

points, in 2 different coordinate space.

14. Using this transformation matrix, the 3D mesh was registered to the kidney phantom, and brought the entire setup and calculations into the NDI coordinate system

- **Arrow shown in RViz for visual aid:** The endoscope can bend in only two directions, and it is in a cylindrical shape, with a cylindrical position sensor attached to it. So, once the whole setup [Fig. 3.8] is insi-

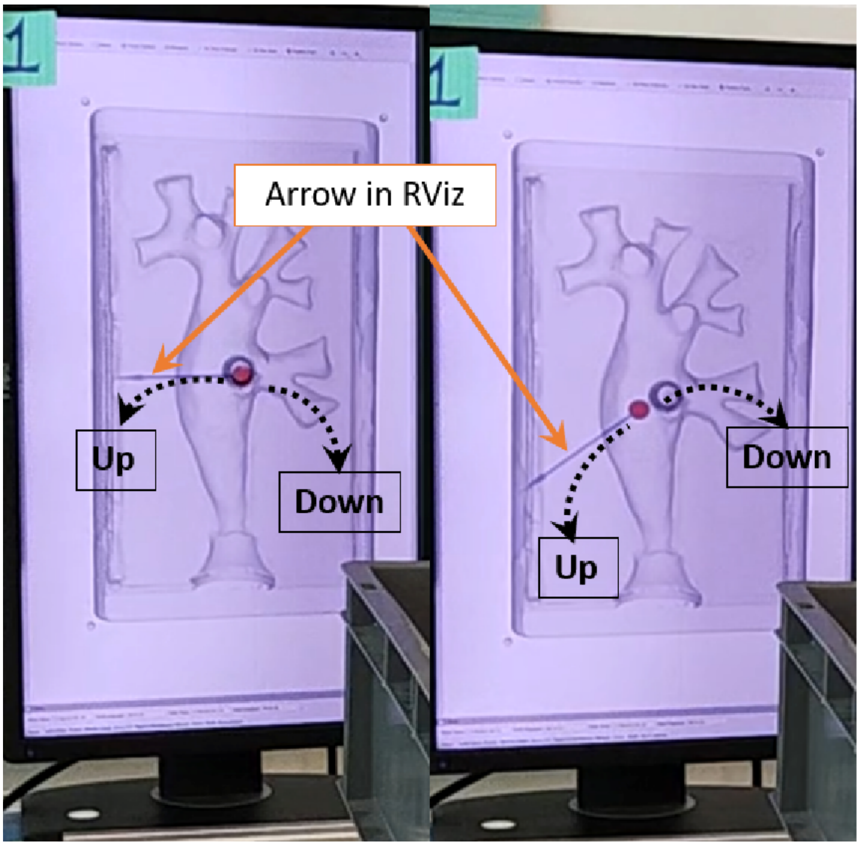

Fig. 3.22: Arrow shows where the endoscope will move, if pressed 'Up' or 'Down'

de the kidney, it is very difficult to estimate without additional test, the expected bending direction of the endoscope.Loss of orientation during endoscopic manipulation remains a persistent challenge, especially when the image plane rotates with the scope while offering no explicit reference to what is anatomically "up." In practice, surgeons often fall back on improvised strategies—such as ejecting a small jet of water and watching its gravitational direction—to infer the dependent side of the lumen. During retrograde intrarenal surgery and flexible ureteroscopy, this difficulty becomes more pronounced: calyces can be visually indistinguishable, the ureteroscope undergoes continuous rotation and deflection, and clinical guidelines explicitly advise establishing the calyceal system's spatial layout before proceeding. These factors create a strong need for additional orientation cues. To mitigate this orientation issue, the methodology introduces an arrow-based visual cue, with a ball marking the endoscope tip; this indicator, displayed on the RViz screen, conveys the real-time direction of the scope.

The arrow in RViz help users navigate by indicating in which direction the endoscope will bend, as shown in Fig. 3.22.

- **Connection between the kidney phantom, the 3D kidney mesh, and em position sensor**: With the registration, the position (in em-sensor coordinate system) of the kidney phantom and the kidney mesh were already saved in a Links and Nodes process. The em position sensor's coordinates were constantly relayed via the NDI Aurora system, captured and stored by a process in Links and Nodes.

- **ImFusion Suite Graphical User Interface (GUI):** Communication between the GUI and the em position sensor was using OpenIGTLink. This enabled the GUI to track the sensor located at the endoscope tip and visualize it within the simulated camera view, as shown in Fig. 3.23

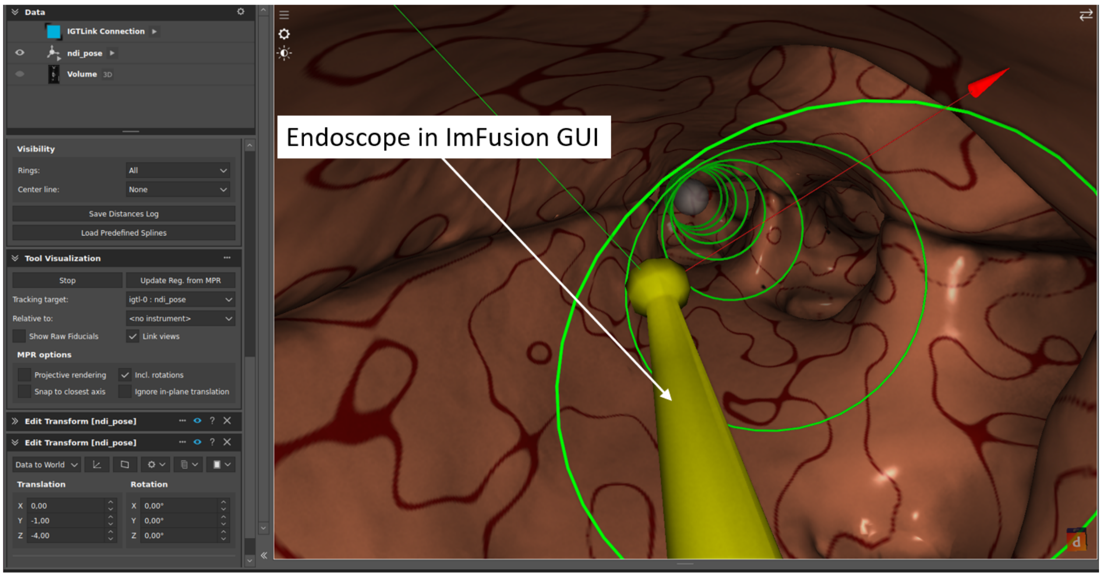

Fig. 3.23: ImFusion GUI with the endoscope visualized inside the simulated camera view.

3.4.3 Setting up the components for Tactile Feedback

One time setup using the Arduino IDE: the FingerTac module was uploaded with a modified version of its Arduino scripts to generate vibration patterns on receiving certain inputs via the Serial Monitor

Once the FingerTac was uploaded with the intended Arduino sketch, its Serial Monitor was accessed using serial communication via Links and Nodes to generate the vibration patterns

3.4.4 Visual Feedback Components

1. **RViz screen**:

Fig. 3.24: The screen showing RViz, with the ball representing the endoscope's tip

a) It will show a global map of the kidney, as shown in Fig. 3.24.

b) Ball on the screen: The real-time location of the endoscope tip is shown as a dynamic ball, moving on the global overview of the kidney. The color of the ball changes between green, yellow, and red, according to how far the operator (endoscope's tip) is from the walls during the exploration phase and the extraction phase, as shown in fig. 3.25

c) Arrow attached to the ball: It will indicate the direction of the bending of the endoscope (Fig. 3.22).

2. **ImFusion screen**:

a) It will simulate the endoscopic camera's view as shown in fig. 3.26, going inside the registered 3D mesh.

b) Stones: There are some simulated stones created inside the 3D mesh

c) Path to the stone: The pre-defined path to each stone is presented as

Fig. 3.25: RViz: the ball represents the endoscope tip, and the color changes according to the distance from the walls of the kidney - *green*: safe distance, *yellow*: borderline-safe distance, *red*: threshold distance, about to collide with the wall

a spline.

d) Rings around the path: There are safety rings for each path, which show the safe space within which users should navigate, with slight deviations from the planned spline.

In the **Exploration phase**, only RViz will be providing the additional features for visual feedback, while the imFusion Suite will show the simulated endoscopic view.

In the **Extraction phase**, both RViz and ImFusion Suite will be active, with ImFusion Suite having the primary features for visual feedback.

3.4.5 Tactile Feedback Components

- **FingerTac**:

  1. The FingerTac is worn on the wrist and the fingers (as shown in Fig. 3.9).

  2. It is wired to the system and is accessed by the serial connection using Links and Nodes

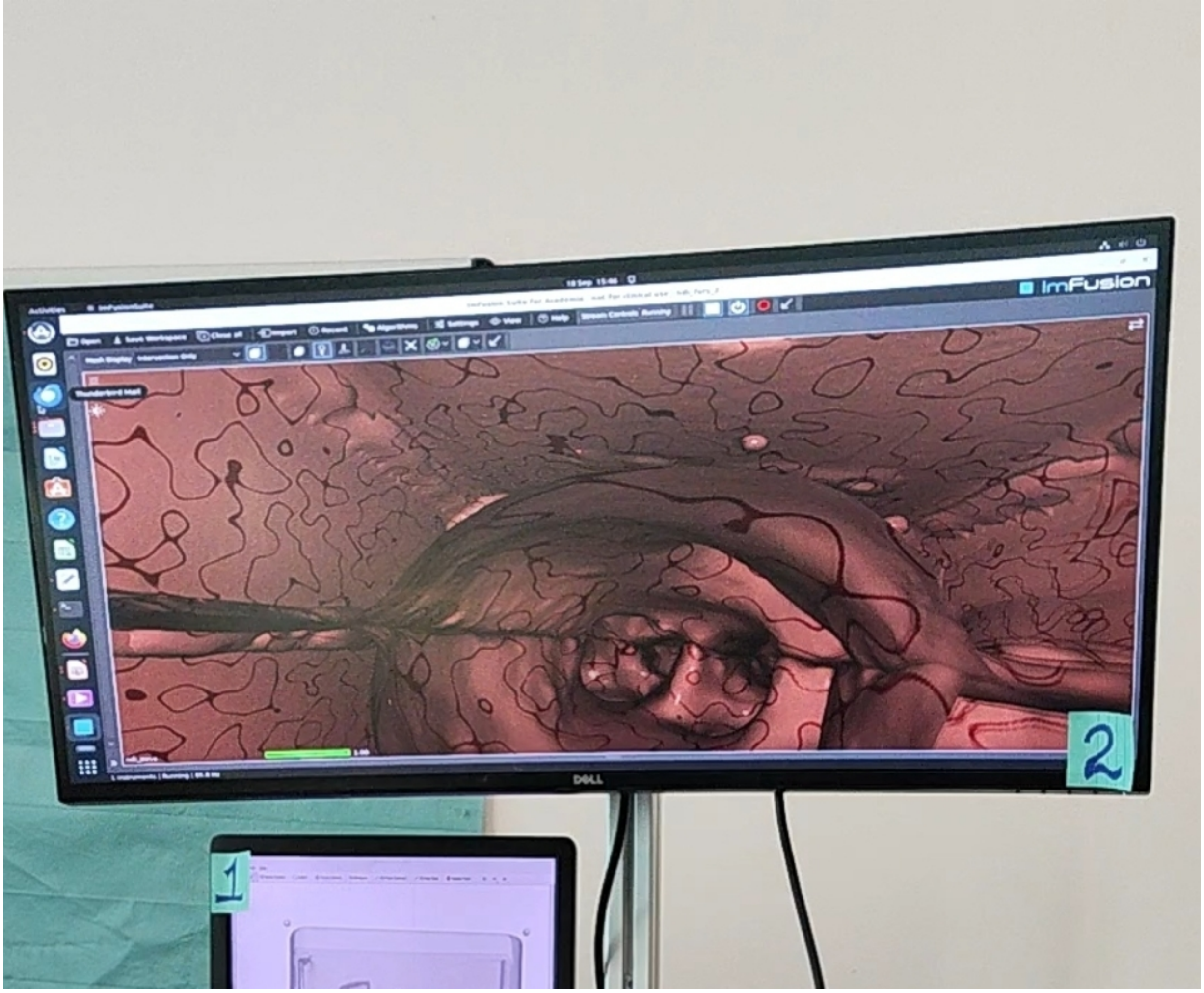

Fig. 3.26: ImFusion screen

3.5 The feedback system

The camera integrated into the endoscope gives a limited visual view, which will be simulated in the imFusion screen (as shown in fig. 3.26).

- **Parameters considered**:

  1. The current phase of the surgery:

     a) Exploration Phase (or) Collision-Avoidance Phase
     b) Extraction Phase (or) Guidance Phase

  2. Modalities activated:

     a) Visual Feedback

b) Tactile Feedback

The feedback modalities are now explained according to the phases in section 3.6 and 3.7. Each phase will have both visual and haptic feedback features described.

3.6 Exploration Phase

The surgery starts with Exploration of the kidney, where the operator uses the camera view for a systematic visual examination of the renal collecting system and ureter, especially the kidney, using the flexible ureteroscope via the urinary tract.
Targets of this step includes assessing the anatomy, and identifying the location, size, number, and composition of stones, to plan the stone treatment/extraction strategy.

Goal:
For the visual feedback modality using RViz (like shown in 3.27), the main goal will be to explore different parts of the kidney, trying to stay away from hitting/touching the walls of the kidney, as much as possible.
The tactile feedback when activated, will alert the patient when they are too close to the walls of the kidney.

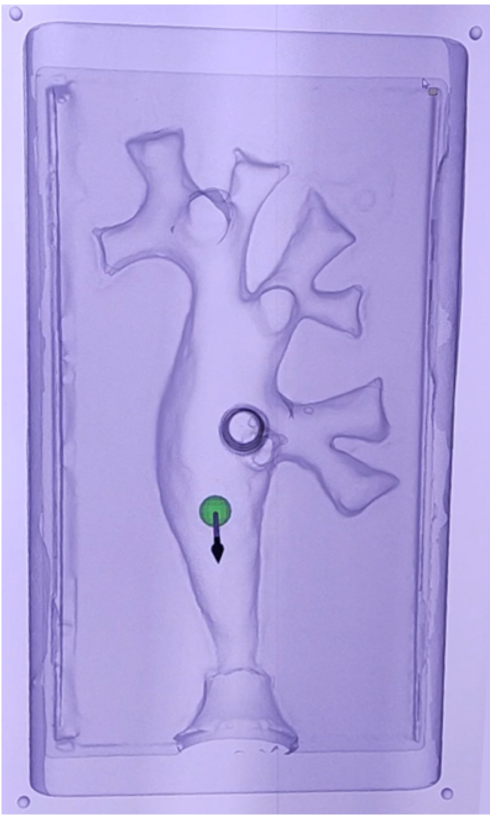

Fig. 3.27: The screen showing RViz, with the ball representing the endoscope's tip and the arrow showing the direction in which the endoscope bends

3.6.1 Exploration Phase - Visual Feedback

- **Active feedback features:** ImFusion will show the endoscopic camera view, without any stones RViz will have the bird's eye view of the kidney, the ball depicting the real-time location of the endoscope tip, and the arrow showing which direction the endoscope will bend [3.22].

- **Computations**: In RViz, the registration of the phantom kidney and the 3D mesh was done as explained in section 3.4.2 The operator not only can use the overview of the kidney to get the current location, but also to understand how the endoscope bends, by using the arrow.

  This way, even if the endoscope is close to touching the walls on the top or bottom of its current position, if the ball is red, and the arrow is pointing exactly up/down, the operator only needs to bend the endoscope in the oppsoite direction without the need to do more complex movements. Since the setup includes two cylindrical bodies - endoscope and position sensor, and the position sensor will always send the position of itself, a circular-fit calibration was carried out to determine the center of this combined setup. The approximate radius of this combined endoscope and em sensor cylindrical module was found to be 2 mm.

  The position sensor was attached to the endoscope such that the +y direction of the sensor was perpendicular to the tangent to the point of contact between the endoscope and the em sensor, as shown in Fig. 4.2. Hence, all the real-time position values: x, y, z coordinates were shifted by 2 mm in the -y direction The arrow showing the orientation of the position sensor was also shifted by 2 mm in the -y direction The ball depicting the shifted coordinates, the 3D mesh, and the arrow were loaded in RViz The closest point on the mesh from the shifted position of the position sensor was calculated, which gave the distance from the walls of the kidney. This distance is compared to a threshold distance set by the user, and used to change the color of the ball, which acts as an additional visual aid for the users, alerting them about possible collisions with the kidney.

- The threshold distance is the minimum distance from the walls of the kidney which will be allowed for the user to go to, without throwing any alerts. For expert surgeons, the threshold can be much lower than for a new trainee.

- Color changes and meanings:

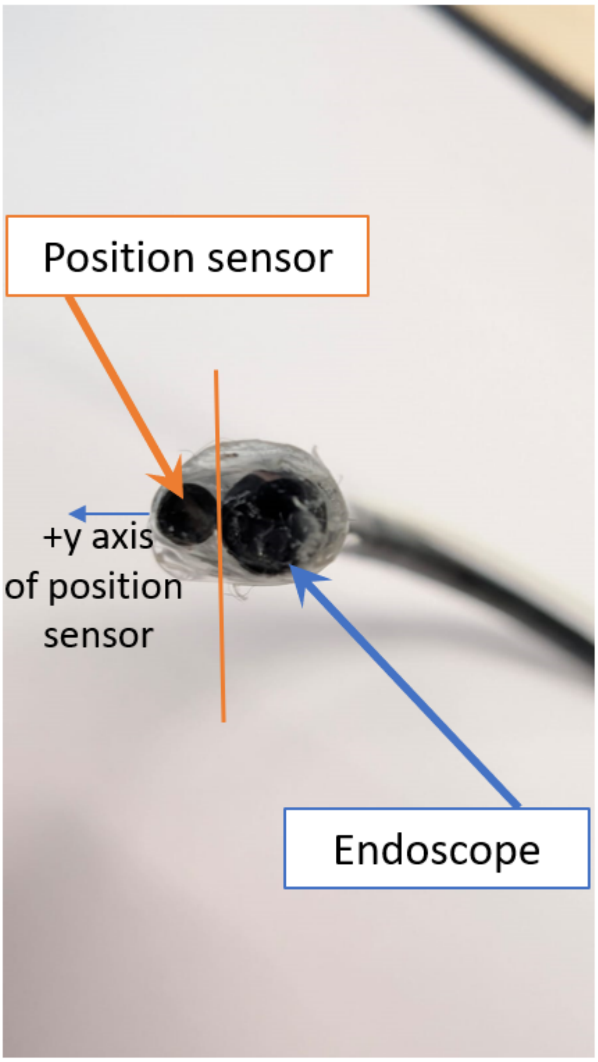

Fig. 3.28: The +y axis of the position sensor was aligned as shown

1. Green: signifies a safe distance from the walls
2. Yellow: means the operator is at a borderline-safe distance (threshold distance set by the surgeon) from the walls
3. Red: implies that the operator is now too close, well within a set threshold of colliding with the walls of the kidney

3.6.2 Exploration Phase - Tactile Feedback

- **Active feedback features:**
  All the Links and Nodes processes, and the process controlling the FingerTac would act according to the process managing the ball in RViz

- **Computations:**

The distance, which is used to change the color of the ball to alert the user about collisions, is also used to trigger vibration patterns. These distances (and subsequently the color of the ball) are sent to the Links and Nodes process, which communicates with the FingerTac using the system's serial monitor

The vibration patterns according to the colors:

1. Green: no vibrations
2. Yellow: mild soft vibrations
3. Red: strong vibrations

3.7 Extraction Phase

- Once the Exploration of the kidney is complete, stone fragments are removed from the urinary tract during the Extraction phase, either directly or after being fragmented by laser lithotripsy or other methods.

- **Goal:**
  For the visual feedback modality using ImFusion and RViz, the main goal will be to reach the virtual kidney stone, by following the pre-planned spline.
  The operator should stay within the safety rings around the spline to avoid hitting the wall.
  The tactile feedback when activated, will alert the surgeon when they are too far from the suggested trajectory.

- RViz will also be available for the users, to warn the surgeon when they are close to the kidney walls.

3.7.1 Extraction Phase - Visual Feedback

- **Active feedback features:**

  1. ImFusion will show the endoscopic camera view, the stone, the pre-planned spline, and the safety rings, as shown in Fig. 3.29
  2. RViz will have the bird's eye view of the kidney, the ball depicting the real-time location of the endoscope tip, and the arrow showing which direction the endoscope will bend

- **Computations:**
  In RViz and ImFusion, the registration of the phantom kidney and the 3D mesh was done as explained in section 3.4.2. The IGTLink was established for communicating with ImFusion GUI to get the distance between

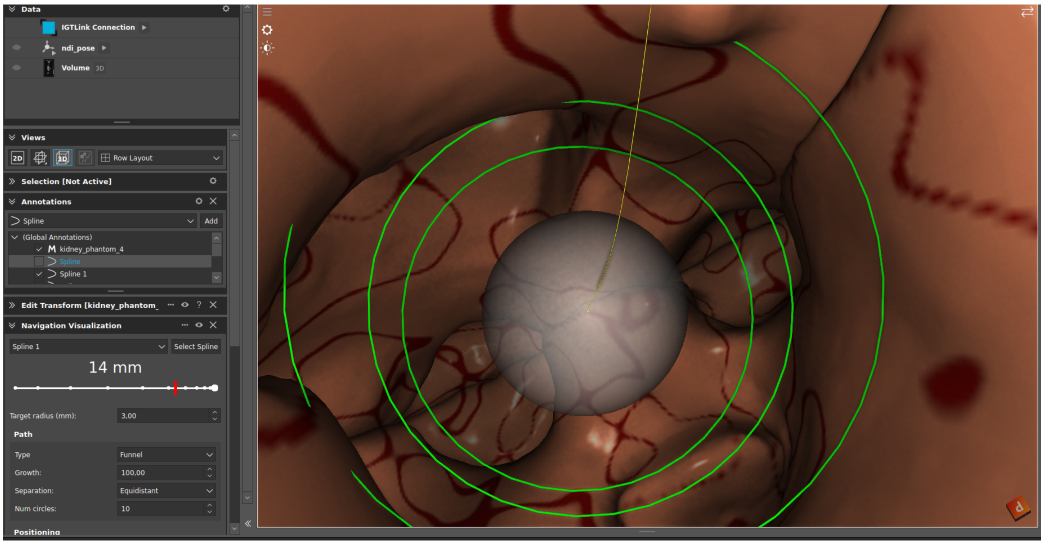

Fig. 3.29: ImFusion Suite GUI: simulated endoscopic view, with the rings indicating the path and the safe volume to navigate and a simulated kidney stone.

the shifted current position's coordinates and the spline to be followed ImFusion was also used to get the distance from the current position to the stone. When this distance was close to zero, it meant the operator has reached the stone.

3.7.2 Extraction Phase - Tactile Feedback

- **Active feedback features:**
  FingerTac: FingerTac would be connected to the system running all the Links and Nodes processes, and the process controlling the FingerTac would act according to the values received from ImFusion

- **Computations:**
  The distance from the spline, if greater than a threshold, will trigger a vibration pattern via the FingerTac. The threshold is also the radius of the safety rings, which can be adjusted before the Extraction phase. The color of the rings changes between green and red, based on how far is the operator

  The vibration patterns according to the colors of the rings in the ImFusion Suite:

  1. Green: no vibrations
  2. Red: strong vibrations

4 Exploratory Study and Conclusion

To evaluate the efficacy of the proposed methodology and assess how the feedback modules influence user experience, an exploratory user study was conducted. The study involved 13 participants representing diverse demographic backgrounds. Among them, seven participants reported moderate to high experience with tele-operation or manipulation systems. Most participants exhibited moderate to high familiarity with visual and haptic feedback systems, whereas only two participants had prior exposure to endoscopic simulation environments. The participants' ages ranged from their early twenties to early fifties.

4.1 The Setup for Conducting the Study

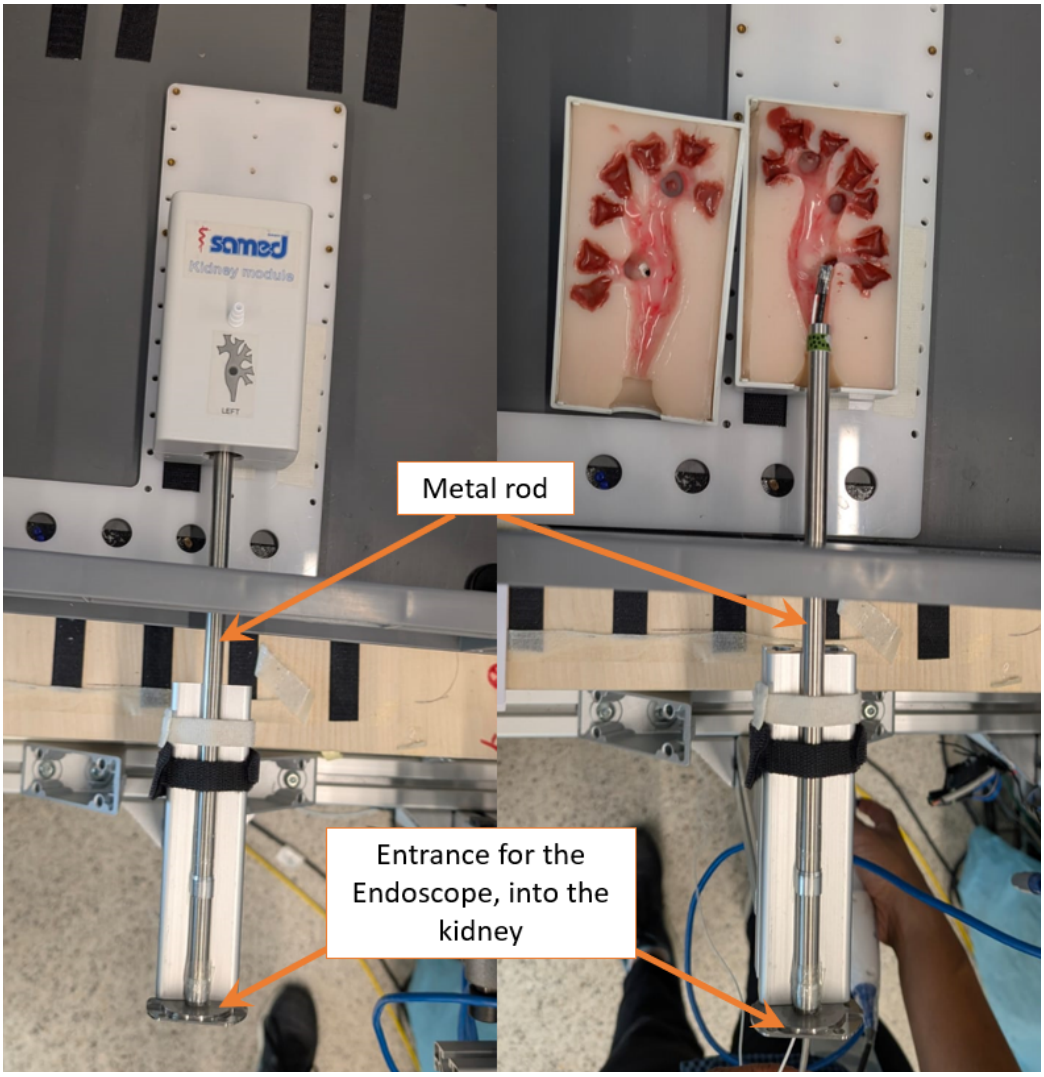

Fig. 4.1: Setup of the kidney phantom

4.1.1 Kidney Phantom and the Endoscope

The em-position sensor was attached to the endoscope, with respect to the orientation of the arrow in RViz, as shown in 4.2. The users would try out operating the endoscope with

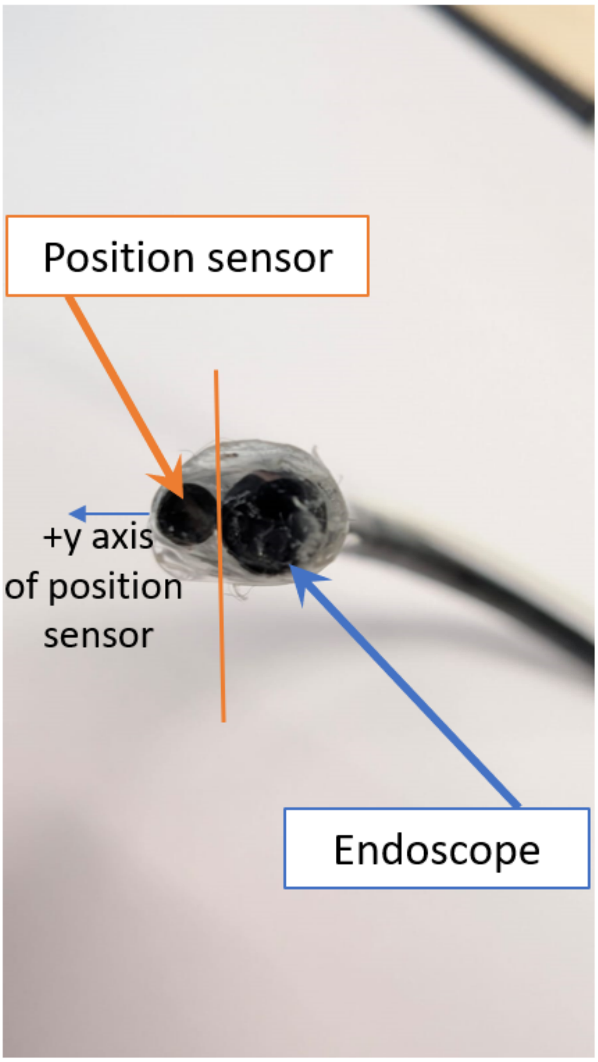

Fig. 4.2: The +y axis of the position sensor was aligned as shown

both their hands, one hand to control the endoscope bending and rotation and the other to push or pull the endoscope and em-sensor in the kidney, as shown in fig. 4.3

The cylindrical module consisting of the endoscope and the sensor was fragile and hence the kidney phantom was set up with a metal rod to simulate the access pathway used during the kidney stone removal procedure to access the kidney, as shown in Fig. 4.1.

The kidney phantom was placed inside the electromagnetic volume, generated by the NDI electromagnetic generator.

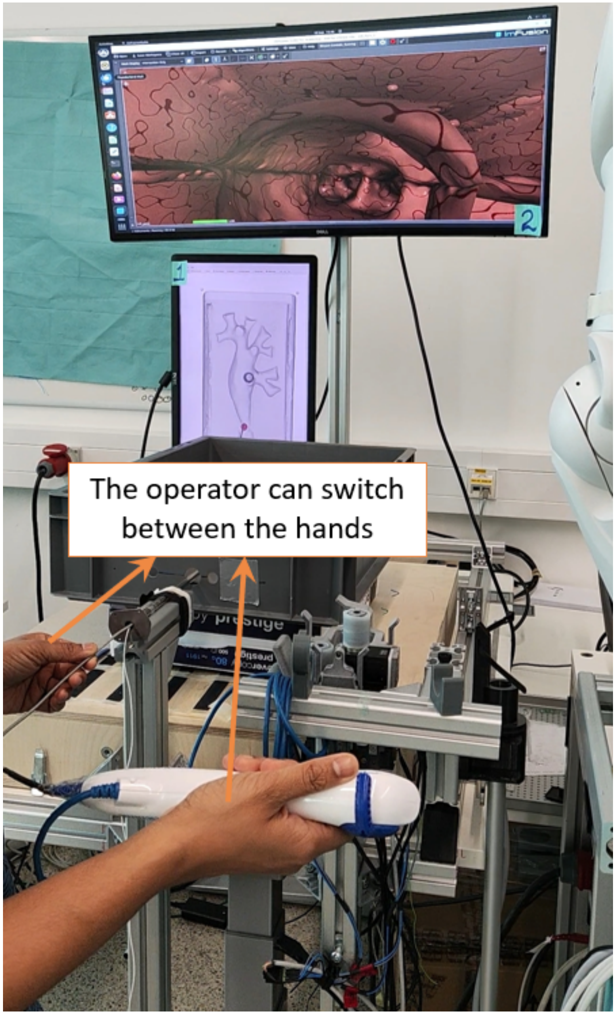

Fig. 4.3: Operator can use either of their hands to hold the endoscope or guide the wire

4.1.2 The Feedback Modules

Both the visual feedback modules were set up on two separate screens as shown in Fig. 4.4

The users were made to wear the FingerTac module on the hand which was used to navigate the endoscope and em-sensor in and out of the kidney, as shown in fig. 4.5.

4.2 Parameters of the Study and Sequence of Steps

The study was conducted for 13 users, in two phases: the Exploration phase and the Extraction phase. There were three feedback modules: no feedback, visual feedback, visual and haptic feedback.

Data were collected from 13 users; however, the data for one user was excluded from analysis due to inconsistent measurements caused by a logging malfunction. Consequently,

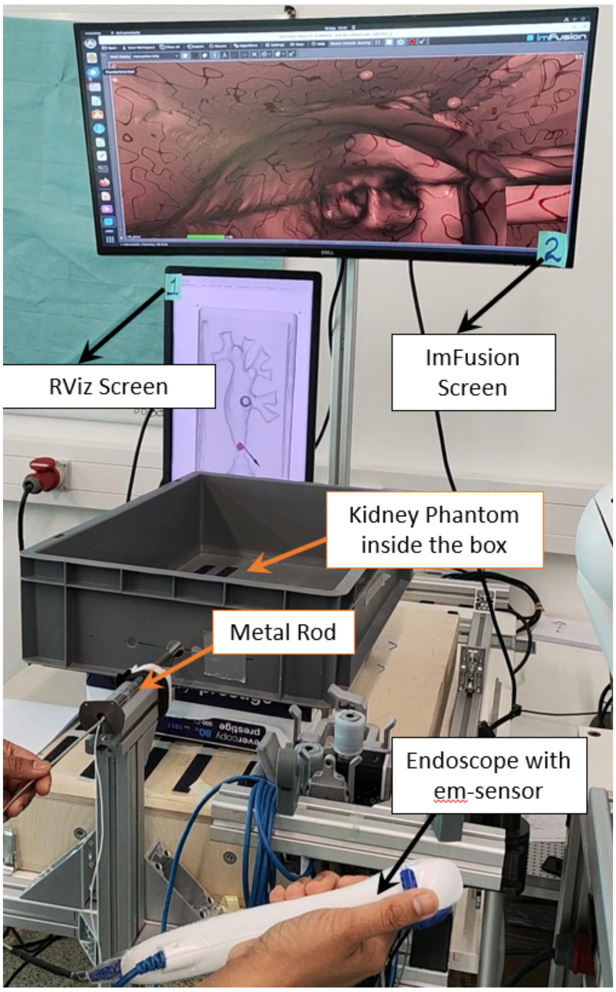

Fig. 4.4: Setup of the both the Visual Modules - RViz on Screen 1 and ImFusion GUI on Screen 2

for the final evaluation, the inputs from 12 valid participants were considered.

Exploration Phase:
During the trials for the exploration phase, the primary goal was to go to a specific calyx, example shown in fig. 4.6, while avoiding collisions with the wall, as much as possible. There were two calyces: one was relatively easier to reach than the other.

Extraction Phase:
During the trails for the extraction phase, the primary aim was to follow the pre-defined path to the stone, again while avoiding collisions with the wall, as much as possible. There were two different 'stones', out of which, one had an easier pre-defined trajectory to follow than the other.

In total, each user had 10 experiments/trials to complete:

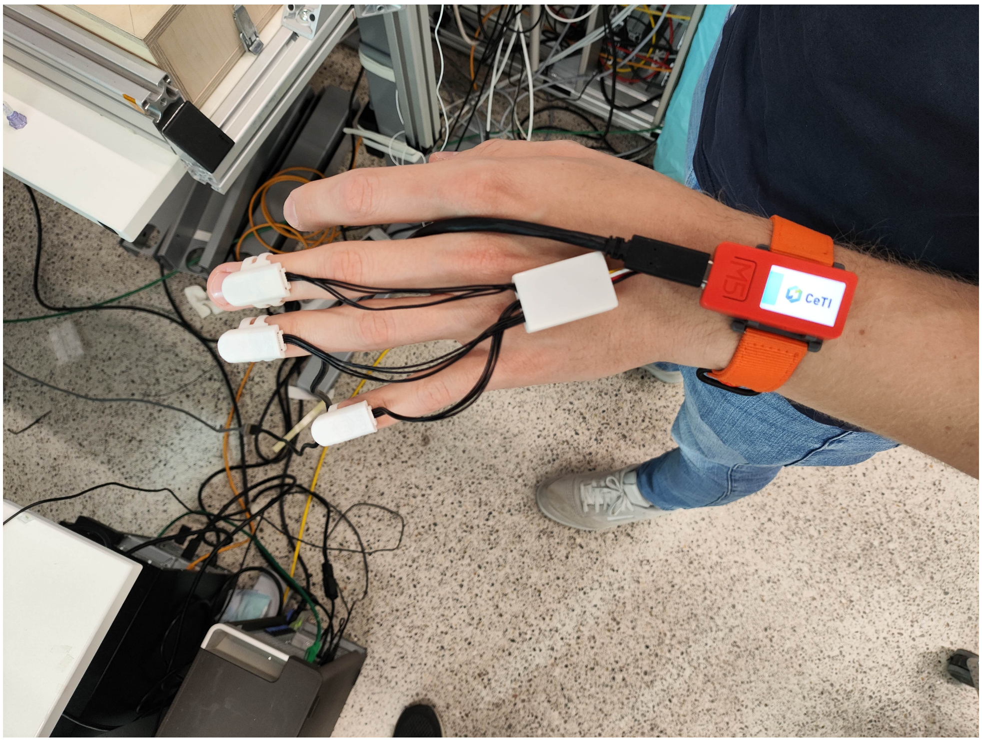

Fig. 4.5: An user wearing the FingerTac

1. The first six trials were always the same:

   - Exploration Phase
     Trial **1**: no feedback - exploration
     Trial **2**: visual feedback - exploration
     Trial **3**: visual & haptic feedback - exploration
   - Extraction Phase
     Trial **4**: no feedback - extraction
     Trial **5**: visual feedback - extraction
     Trial **6**: visual & haptic feedback - extraction

2. The last four trials were varied, in the a random combination of:
   Visual-exploration, visual & haptic- exploration, visual-extraction, and visual & haptic- extraction

3. The last four trials had the harder calyx and stone to reach.

By adapting this three-variant paradigm to flexible ureteroscopy tasks, the experiment can compare user performance and learning across increasing levels of sensory assistance [Aji23].

The table 3.1 shows the sequence given to each user, with the coding mechanism according

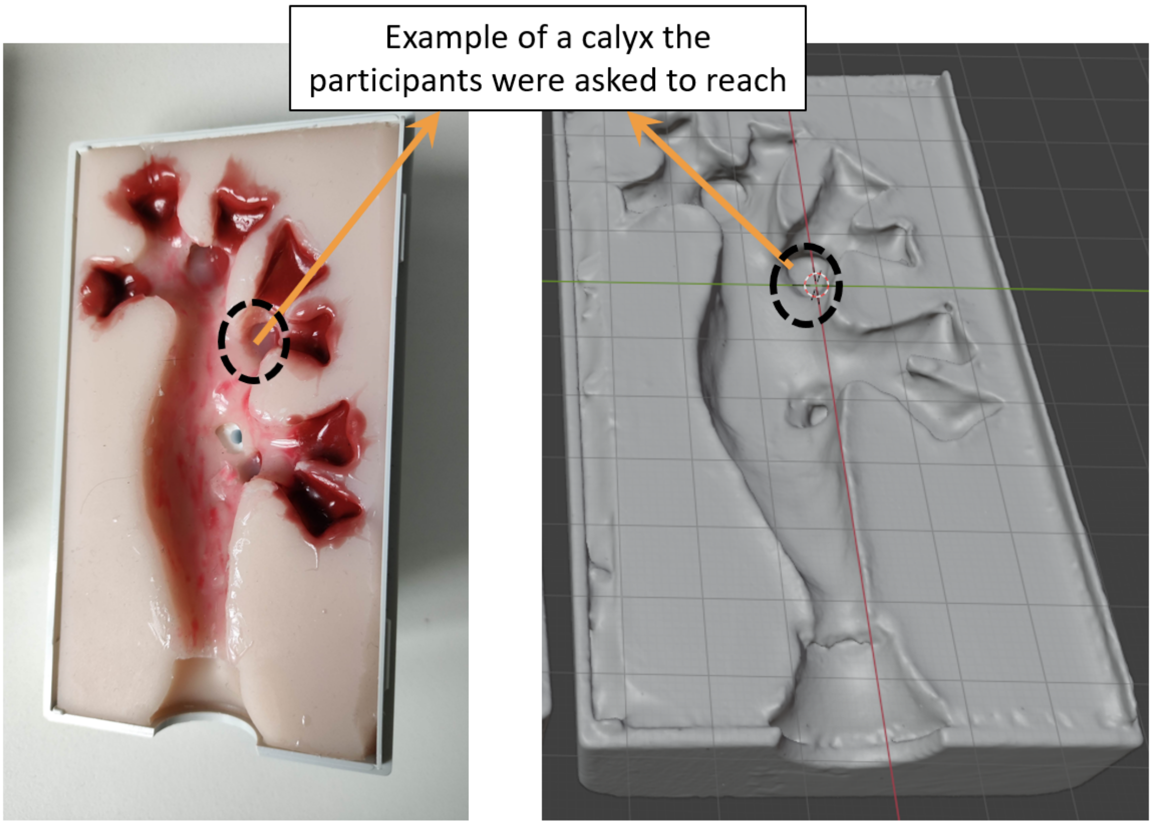

Fig. 4.6: Example of a calyx the participants were asked to reach

to the following:

- **1**: no feedback
- **2**: visual feedback
- **3**: visual & haptic feedback
- **A**: Exploration
- **B**: Extraction

To mitigate learning and order effects, participants were assigned one of four pre-defined feedback sequences (codes 1–4, according to four distinct sequences), each representing a distinct ordering of the three feedback conditions: no feedback (1), visual feedback (2), and visual & haptic feedback (3). The randomized design ensured that no two consecutive participants experienced the same sequence of feedback modes (e.g., 123A–123B–23A–23B or 123A–123B–23B–23A). This counterbalancing prevented bias due to progressive familiarization with the task, across users.

Participants 9–13 were provided with an extended warm-up phase prior to the experimental trials to allow them to become better accustomed to the setup. This was implemented to evaluate the effect of increased familiarization on task performance.

Tab. 4.1: The Sequence of Steps - According to the User: '1': no feedback, '2':visual feedback, '3':visual & haptic feedback, 'A':Exploration, 'B':Extraction

User	Sequence	code
2	123A-123B-23A-23B	1
3	123A-123B-32B-23A	2
4	123A-123B-23A-23B	1
5	123A-123B-32A-23B	3
6	123A-123B-23B-23A	4
7	123A-123B-23A-23B	1
8	123A-123B-23B-23A	4
9	123A-123B-23A-23B	1
10	123A-123B-23B-23A	4
11	123A-123B-23A-23B	1
12	123A-123B-23B-23A	4
13	123A-123B-23A-23B	1

4.2.1 Steps

1. Users were given a small introduction to fURS, robot-assisted surgeries, and the overall idea behind this study. Then, they were asked to fill the demographics questionnaire, with a pseudonym, to anonymize their answers.

2. Once all the hardware was introduced to the user, the bending of the endoscope in two directions were shown to the user and a few minutes were given as a warm-up phase for the user to try out the endoscope, its movement inside the kidney, the synchronization between the visual feedback modules and the tactile feedback system.

   NOTE: Whenever the user was in 'no feedback' trial, only the imFusion Suite GUI was active, without any additional rings or path, to simulate the endoscopic camera view. When the user received only visual feedback, RViz was switched on, with the ball corresponding to the endoscope tip, the changing colors of the ball and the arrow. ImFusion GUI (without any additional rings or path) simulated the endoscopic camera view. With visual & haptic feedback, the rings to simulate the predefined path was switched in the ImFusion GUI, apart from all the features available in RViz.

3. After the 'no feedback' trial, one round of exploration phase (visual feedback, and visual & haptic feedback) was conducted. In this phase, the simulated stone was not shown in the ImFusion GUI.

4. In the extraction phase, only the simulated stone was shown additionally in ImFusion

GUI.

4.3 Results

Data were collected from 13 users; however, the data for one user was excluded from analysis due to inconsistent measurements caused by a logging malfunction. Consequently, the results reported below are based on 12 valid participants.

To evaluate the impact of feedback modalities on user performance, valid data from 12 participants were analyzed across three conditions: No Feedback (baseline), Visual Feedback, and Visual & Haptic Feedback.

4.3.1 Exploration Phase

For each trial, three task performance metrics were extracted:

1. R% (Red colored values) — proportion of instances where the user was very close to the wall or collided with the walls of the kidney

2. Y% (Yellow colored values) — proportion of instances where there was a moderate distance from the wall

3. G% (Green colored values) — proportion of instances where the user was at a considerably safe distance away from the wall

Fig. 4.7: Results comparing feedback modules for the Exploration Phase

Here, R%, Y% and G% were considered and results are plotted in Fig. 4.7.

Analysis of participant performance across trials revealed distinct trends across all three metrics—R%, Y%, and G%. Overall, users exhibited a reduction in R% (instances of contact or near-collision with kidney walls) from approximately 32–35% in early trials to below 15% in later sessions, accompanied by an increase in G% (stable, safe distance) from roughly 35–40% to 65–75%, indicating progressive stabilization and improved control. The proportion of Y% (moderate proximity to collision) remained moderate (typically 25–45%) but declined steadily as users adapted to the task. Participants such as Users 6, 10, 11, and 13 achieved high G% (>80%) with minimal R%, demonstrating proficient and consistent operation. Others (e.g., Users 4 and 5) showed steady gains, while Users 7–9 exhibited greater variability.

Importantly, Users 9–13, who were provided with additional acclimatization time, showed improved baseline stability and faster transition toward high G% values in their initial trials, suggesting that pre-exposure to the system reduced early-stage learning noise. Performance improvements were otherwise consistent across feedback-sequence codes, indicating that multimodal feedback, rather than task order, primarily drove enhanced precision and stability.

4.3.2 Extraction Phase

Deviations from the pre-defined Splines (from the entrance to the Stones):

For the deviations, under each trial, two task performance metrics were extracted:

1. R% (Red colored values) — proportion of instances where the user deviated far, more than the given threshold, from the predefined trajectory

2. G% (Green colored values) — proportion of instances where the user was within the threshold distance from the trajectory

As seen from the results shown in fig. 4.8, across all participants and feedback modes, the data show a progressive reduction in error rate (R%) and a corresponding increase in stability (G%) as feedback richness and user familiarity increased. On average, R% decreased from about 55–60% in the no-feedback baseline to approximately 45–50% under the first visual feedback, and further to 35–40% with visual + haptic feedback. By the second repetition of each feedback condition (last four trails), participants either maintained or improved their performance, with several achieving G% values above 80%, indicating stable and controlled navigation. This trend highlights a consistent learning and adaptation effect, where users integrated multimodal cues to minimize contact and maintain safer trajectories.

Despite increased task complexity in the later trials, most participants sustained or enhan-

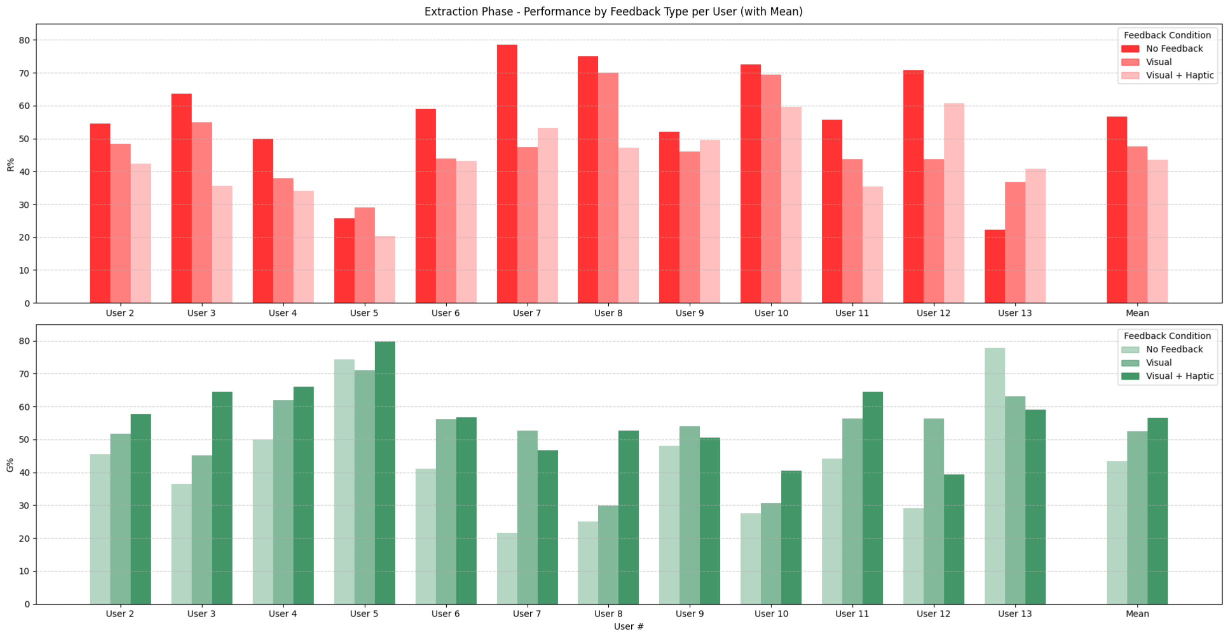

Fig. 4.8: Deviations from Path according to the different feedback modules

ced performance, suggesting transfer of learned control strategies across difficulty levels. Notably, Users 6, 11, and 13 exhibited substantial improvements, reducing R% by over 50% and achieving consistently high G% (>75%) in later trials. User 4, who performed the harder trajectory first, initially showed higher R% values but achieved comparable stability in later easier trials, indicating robust feedback adaptation independent of task order.

Overall, these findings confirm that multimodal feedback (visual + haptic) significantly improved user precision and confidence compared to visual-only or no-feedback conditions. Participants who received extended familiarization (Users 9–13) displayed higher baseline stability and smoother learning curves, demonstrating that even brief pre-exposure can enhance early-stage performance. Collectively, the results highlight the combined influence of feedback richness, repeated exposure, and user acclimatization in promoting safe, efficient, and consistent control of the endoscope.

Collisions with the walls of the kidney in Extraction Phase

For collision-avoidance, under each trial, three task performance metrics were extracted:

1. R% (Red colored values) — proportion of instances where the user was very close to the wall or collided with the walls of the kidney

2. Y% (Yellow colored values) — proportion of instances where there was a moderate distance from the wall

Fig. 4.9: Results comparing feedback modules for the Extraction Phase

3. G% (Green colored values) — proportion of instances where the user was at a considerably safe distance away from the wall

The results are plotted in fig. 4.9. Across all five trials per participant—including the baseline (no feedback), two visual-feedback, and two visual + haptic-feedback trials—participants demonstrated clear improvement in control precision and spatial stability. R%, representing near-collisions or wall contact, steadily decreased from around 30% in the no-feedback condition to below 15% in the final sessions. G%, indicating safe and stable navigation, increased from roughly 30–40% to over 65–70%, while Y% (moderate proximity) narrowed over time, suggesting growing user confidence and decisiveness. These results confirm that participants progressively adapted to the task dynamics, reducing critical errors and maintaining safer trajectories as multimodal feedback was introduced.

Task difficulty also influenced performance: Set 1 (Trails 5 and 6) involved easier trajectories, while Set 2 (two of the last four trials) required tighter, more complex movements. Despite this increase in difficulty, participants largely maintained or improved their performance, demonstrating transfer of learning between task complexities. User 4, who completed the harder task first, initially showed higher R% but rapidly improved on the easier set—indicating that early exposure to challenging conditions may accelerate learning once feedback cues are internalized.

Participants who received additional familiarization time (Users 9–13) exhibited smoother early performance, lower baseline R%, and smaller fluctuations across trials. This suggests that even brief pre-task acclimatization enhances early-stage control and reduces learning lag. Overall, the results highlight that feedback richness (visual + haptic), task repetition, and prior familiarization collectively improved operational accuracy, confidence, and stability in teleoperated navigation.

4.4 Evaluation of NASA-TLX inputs

4.4.1 Overall comparison of the feedback modules

Across both phases, Visual Feedback consistently produced the lowest workload (exploration phase = 4.69, extraction phase = 4.73), showing that participants found purely visual cues the most comfortable to use. This trend is clearly reflected in the horizontal NASA-TLX profile (fig. 4.10), where Visual Feedback shows uniformly lower bars across most workload dimensions compared to the other modules. The No Feedback condition was the most demanding in both phases, with the highest frustration (5.86 during the exploration phase) and overall workload (5.07 during the exploration phase). Interestingly, extraction phase scores were generally lower than exploration phase for most modules—particularly for No Feedback, where overall TLX dropped from 5.07 → 4.53. This suggests a learning or adaptation effect, where users became more efficient with task repetition.

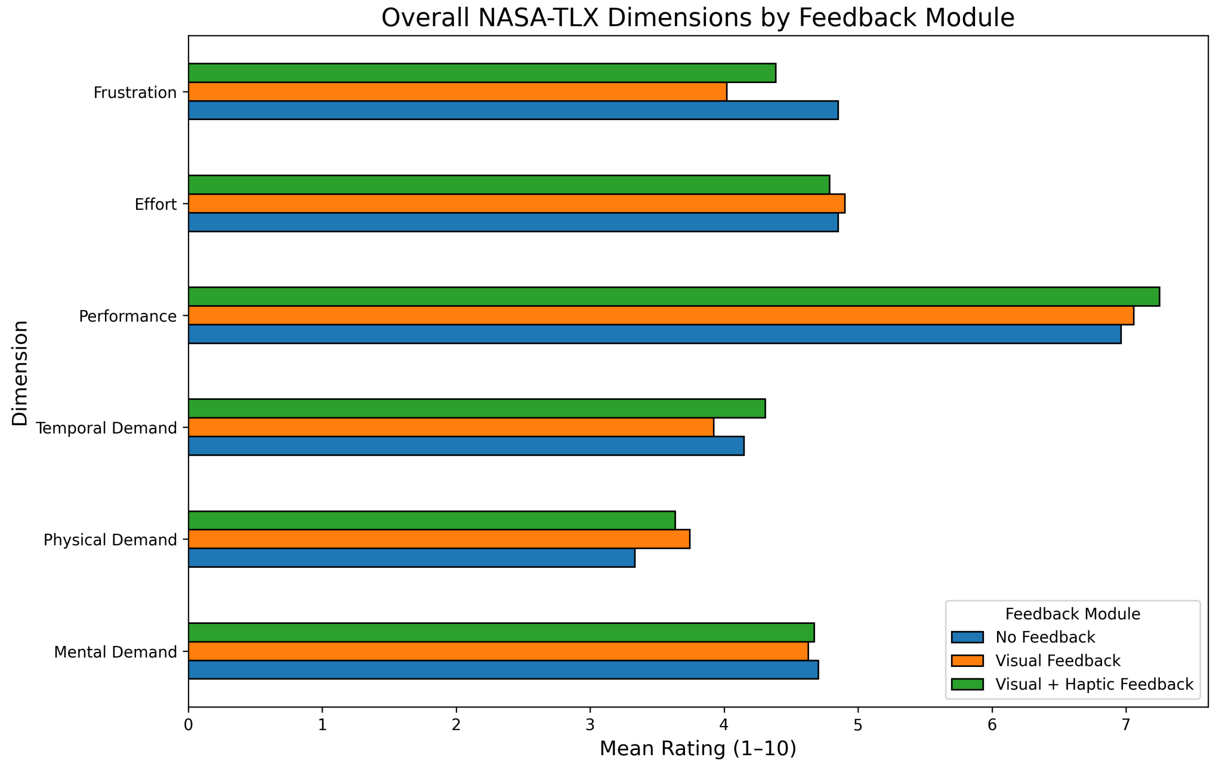

Fig. 4.10: NASA TLX inputs: Results comparing feedback modules for the whole experiment

Performance improved markedly from exploration phase to extraction phase across all modules (e.g., No Feedback: 6.14 → 7.85), showing users' growing familiarity. Frustration also declined in extraction phase, especially under No Feedback (5.86 → 3.77), reinforcing that early exposure may have caused initial strain that eased over time.

When comparing feedback types:

- Visual Feedback → consistently lowest frustration (exploration phase: 4.12, extraction phase: 3.93).
- Visual & Haptic → highest perceived performance (exploration phase: 7.13, extraction phase: 7.34) but slightly higher mental/temporal demand due to dual-sensory integration.
- No Feedback → highest workload and lowest performance initially, improving only after experience.

4.4.2 Goals of Exploration Phase: reaching the right calyx and avoiding colliding with the walls

Comparison of feedback modules:
Participants felt that Visual & Haptic feedback was more effective in avoiding collisions — suggesting that the tactile cues enhanced spatial awareness. This pattern is clearly reflected in the NASA-TLX workload plot for the exploration phase (fig. 4.11), where Visual Haptic feedback shows the lowest physical and temporal demand and the highest performance among the three modules.

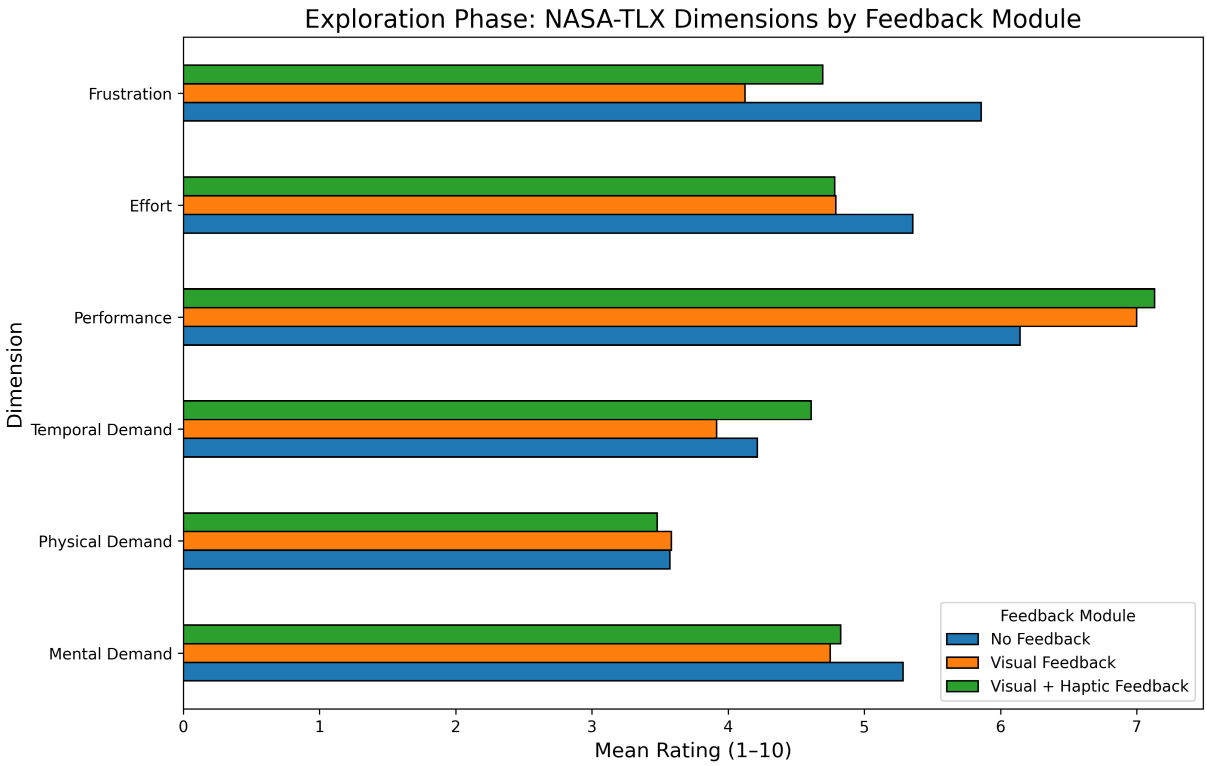

Fig. 4.11: NASA TLX inputs: Results comparing feedback modules for the Exploration phase

However, pure Visual feedback helped more in reaching the target, likely because prolonged visual cues supported precise navigation. Both modules outperformed the No Feedback baseline, confirming that feedback aids performance, but in different ways — haptics improve safety, visuals improve accuracy. Hence, the combination of both feedback types yielded the highest perceived collision avoidance.

Changing color of the user's position (ball):
The color-change cue was the strongest performer overall — participants rated it highly both for collision avoidance and target guidance.

Real time direction (arrow) of the endoscope tip:
The low ratings for real-time direction cues likely reflect users' inexperience rather than the irrelevance of directional information. In endoscopic procedures, loss of orientation is a well-documented challenge—novices often struggle to interpret direction and rely on simple techniques such as squirting water through the channel to infer the lumen's position. Studies such as [RSC+15] emphasize that directional awareness is critical for safe navigation, and effective visual cues or training are needed to make such feedback intuitive for beginners.

Vibrations via tactile feedback system:
Among haptic features, vibration strength performed slightly better than vibration patterns in helping avoid collisions. The vibrations moderately useful for reaching targets indicating that haptic cues primarily serve as warning or alert mechanisms rather than guidance aids.

4.4.3 Goals of Extraction Phase: following the predefined path accurately and avoiding colliding with the walls

Comparison of feedback modules: Since these trials were conducted after users were accustomed better to the system during the exploration phase, participants rated all feedback types highly. This trend clearly is shown in the Extraction-Phase feedback comparison chart (fig. 4.12), where all modules show uniformly high mean ratings and Visual + Haptic feedback leads for path-following tasks. Visual & Haptic feedback now performed best for following the path, showing that with experience, users could integrate visual and haptic cues more effectively.

For reaching the target, imFusion screen visual feedback was rated highest, followed by RViz screen alone, suggesting that improved display layout or clarity directly aided end-point accuracy.

The rings around the path and their changing colors:
The rings and dynamic color cues were rated highest overall, confirming that continuous visual proximity indicators are intuitive and effective once users understand the task.

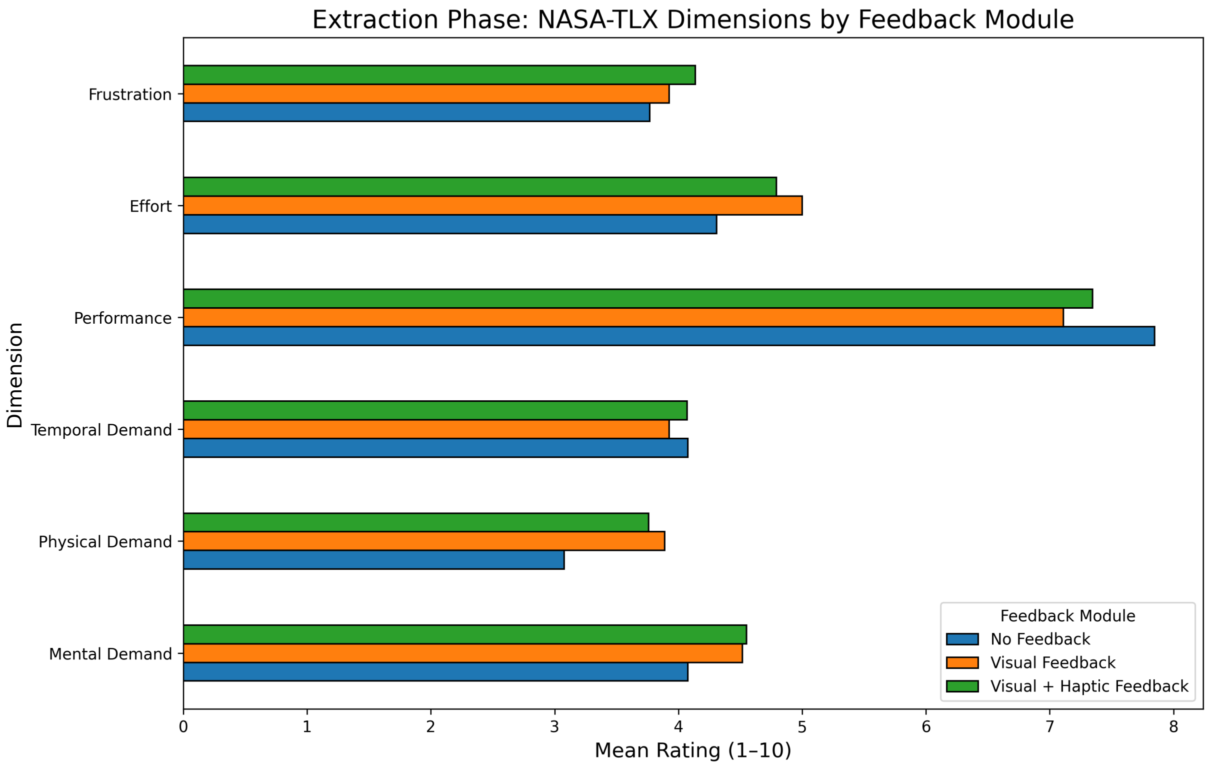

Fig. 4.12: NASA TLX inputs: Results comparing feedback modules for the Extraction phase

Vibrations via tactile feedback system: Haptic feedback played a supporting, not dominant, role in the extraction phase. Vibration strength was the most appreciated, indicating that users valued intensity cues over pattern or duration. After gaining familiarity, users relied more confidently on visual cues while treating haptic alerts as situational reinforcements rather than primary navigation tools.

4.5 Discussion

The user study demonstrated that feedback modality plays a decisive role in shaping user performance, learning behavior, and perceived control during teleoperated navigation. Across all participants, the introduction of augmented sensory feedback - first visual, then combined visual & haptic, produced systematic reductions in collisions with the wall or deviations from the path, and improvements in task performance and completion in both the the exploration and the extraction phase. In the no-feedback condition, participants relied primarily on indirect motion cues, resulting in frequent near-collisions and higher trajectory variability. The addition of visual feedback improved spatial awareness by providing real-time positional context, leading to fewer boundary contacts and smoother movements. When haptic cues were introduced alongside visual information, participants exhibited the lowest error frequencies and the highest stability, indicating that multimodal integration enhances both precision and confidence during teleoperation.

Repeated exposure to each feedback mode revealed a retention and transfer effect: users not only improved within a feedback type but also maintained stable control when transitioning to harder trajectories. This finding suggests that sensory-motor learning generalized across task complexity, with participants internalizing the mapping between multimodal cues and spatial constraints. The visual & haptic feedback condition, in particular, enabled faster adaptation and more consistent performance across repetitions, supporting the hypothesis that haptic reinforcement strengthens visuomotor learning by providing continuous corrective feedback during motion execution. Even as the calyx or trajectory difficulty increased in the later sets, most participants sustained or improved their performance, underscoring the robustness of multimodal guidance.

Individual differences further clarified these effects. Participants 9–13, who received extended familiarization time before the trials, began with higher baseline stability and exhibited smoother performance curves, confirming that pre-task acclimatization significantly shortens the learning phase. Conversely, participants without extended warm-up required more trials to stabilize their motion control, highlighting the importance of training or calibration phases in real clinical or robotic contexts. User 4, who performed the harder trajectory first, achieved comparable final performance to peers, suggesting that feedback quality can offset initial task difficulty when multimodal cues are available.

Collectively, these results demonstrate that multimodal feedback systems combining visual and haptic information offer measurable benefits for teleoperated or robotic navigation tasks. They not only reduce error frequency but also promote consistent spatial awareness and user confidence across repeated and complex tasks. In conclusion, the study confirms that enhanced feedback design and structured familiarization are critical to achieving reliable, precise, and intuitive teleoperation performance.

5 Future Scopes

5.1 Possible Future Extensions/Work

This methodology can be used as a plug and play solution across different endoscopic procedures, and can be extended to build a simulation and training module for medical professionals. A few other extensions are discussed below:

1. **Easier control over activating-deactivating the alerts:**
   The visual and tactile alerts are controlled by separate processes in the system, on the primary desktop. For example, the color of the ball, which changes according to how close the endoscope is to the wall, is operated by a single process and can be turned off by stopping the process.

   So, the option to override the alerts or pause them is currently on the primary desktop and another person needs to select it for the surgeon. This capability can be integrated as a switch into the endoscope handle or the FingerTac wearable module, to let the surgeon decide when the alerts will stop or pause.

2. **Marking real time location of kidney stones:**
   While in the exploration phase, the surgeon can analyze the current number and location of the kidney stones, which might be different from the ones recorded in the pre-operative scans, as sometimes stones shift within the kidney or fragment on their own into smaller pieces. Once the surgeon is near the location of a stone, the coordinates of that location can be marked and saved using the main system or an integrated switch (as mentioned in the previous point (1)). Then, at those locations, stones can be showed in simulation or in RViz as reference points during the extraction phase.

   And additional feature can be introduced, which allows surgeons to use an integrated switch (as mentioned in the previous point (1)) to select other locations, and in turn coordinates, storing them to come back to - where they feel is important for a re-evaluation of the kidney, or to add the locations to the spline - where they select the location for a new stone fragment, not present in pre-operative patient scans.

3. **Dynamic automatic splines for the Extraction Phase:**
   During the exploration phase, the coordinates of the endoscope's tip were recorded along with the timestamp. These coordinates corresponded to the position where the surgeon navigated to, and the timestamp can show how long the surgeon stayed at a particular location. These locations indicate the space in which the surgeons can and prefer to move, and the accumulated timestamps can show the areas of interest. These findings can be used to create dynamic splines for the Extraction phase, which will be easier and unique to each surgeon and each patient.

4. **Bio-impedance sensors for dynamic shape of the kidney:**
Bio-impedance sensing measures the electrical impedance of biological tissue on the application of small alternating currents. As an internal organ (like the kidney) changes its shape or volume, the distribution of impedance across electrode pairs also changes. There are recent advancements including a system and method for guiding a catheter or other medical device to a desired target destination within the vasculature of a patient via bio-impedance measurements [ref: [HCB14]]. A flexible endoscope integrated with a bio-impedance sensor can be used to track organ deformation and local tissue interaction.

5. **Threshold distances according to the geometry of the kidney:**
In the current methodology, to generate the alerts, the threshold distances for both the exploration phase - minimum distance before colliding with the wall, and the extraction phase - maximum deviation allowed from the trajectory, are user defined, but static.

   These thresholds can be dynamically allotted according to the geometry of the hollow space inside the patient's body. It can be calculated as a percentage of the total space available, according to the endoscope's current location.

6. **Replacing 3D mesh reconstruction from the CT scans and the em-sensor with SLAM:**
In the proposed approach a registered 3D mesh, obtained via laser scan of a kidney phantom or as a CT scan of a real kidney, and a 3D position, obtained by an em-sensor, are needed. For kidney stone removal, a non-contrast CT scan is performed before the operation to locate the stones in the kidney. In this type of CT scans it's difficult to differentiate the kidney calyxes, being difficult to register the endoscopic view with the CT scan. To substitute the pre-operative data and the em-sensor. A SLAM algorithm could be use to provide the point cloud of the kidney and the position of the ureteroscope without the need of extra data or extra sensors.

6 Conclusion

This thesis presented the design, implementation, and evaluation of a modular multimodal feedback framework for enhancing navigation in flexible ureteroscopy (fURS). The developed system integrates visual and haptic feedback modalities to improve spatial awareness, reduce cognitive workload, and enhance user performance during minimally invasive endoscopic procedures.

Through iterative experiments with novice and intermediate users, the study demonstrated that haptic augmentation significantly improves navigation accuracy and task completion efficiency, particularly during complex trajectory following and collision-avoidance tasks. NASA-TLX evaluations revealed a consistent reduction in perceived workload and frustration with combined visual-haptic feedback compared to visual-only guidance, confirming the ergonomic and cognitive benefits of multimodal assistance.

The modular nature of the proposed feedback system ensures seamless integration with both robotic and manual ureteroscopic platforms, without requiring additional dedicated hardware. By combining visual and haptic modules into a unified multisensory framework, the system supports more intuitive navigation and reduces the cognitive effort typically associated with endoscopic orientation. The directional arrow displayed in the RViz screen and the proximity-ring indicators in the imFusion screen supply complementary spatial cues that help users interpret scope orientation and surrounding anatomy more rapidly. These multimodal cues collectively contribute to smoother task execution, shorter operative times, and potentially faster patient recovery. Insights from the phase-wise analysis further highlight that haptic feedback is particularly valuable during the early learning curve, improving spatial orientation and operator confidence as users familiarize themselves with the system..

Overall, this research contributes a validated, adaptable framework that can enhance the safety, efficiency, and intuitiveness of future robot-assisted endourological systems. Future work may focus on real-time integration with intraoperative imaging, organ-motion compensation, and adaptive feedback strategies based on surgeon skill level and procedural context.

Literaturverzeichnis

[AAC+25a] Acar, Ayberk ; Atoum, Jumanh ; Connor, Peter S. ; Pierre, Clifford ; Lynch, Carisa N. ; Kavoussi, Nicholas L. ; Wu, Jie Y.: NAVIUS: Navigated Augmented Reality Visualization for Ureteroscopic Surgery. In: *arXiv preprint* arXiv:2503.17511 (2025). `http://dx.doi.org/10.48550/arXiv.2503.17511`. – DOI 10.48550/arXiv.2503.17511

[AAC+25b] Acar, Ayberk ; Atoum, Jumanh ; Connor, Peter S. ; Pierre, Clifford ; Lynch, Carisa N. ; Kavoussi, Nicholas L. ; Wu, Jie Y.: NAVIUS: navigated augmented reality visualization for ureteroscopic surgery. In: *International Conference on Medical Image Computing and Computer-Assisted Intervention* Springer, 2025, S. 433–443

[AAEN+19] Alhunaidi, Omar ; Ahmad, Abdulrahman A. ; El-Nahas, Ahmed R. ; Akroof, Bader ; Alamiri, Ali ; Al-Ajrawi, Feras ; Al-Terki, Abdullatif ; El-Shazly, Mohamed: Impact of case volume per year on flexible Ureteroscopy practice: an internet based survey. In: *BMC urology* 19 (2019), Nr. 1, S. 134

[AD09] Aron, Monish ; Desai, Mihir M.: Flexible robotics. In: *Urologic Clinics of North America* 36 (2009), May, Nr. 2, S. 157–162, viii. `http://dx.doi.org/10.1016/j.ucl.2009.02.001`. – DOI 10.1016/j.ucl.2009.02.001

[AHB+24] Awedew, Atalel F. ; Han, Hannah ; Berice, Bétyna N ; Dodge, Maxwell ; Schneider, Rachel D. ; Abbasi-Kangevari, Mohsen ; Al-Aly, Ziyad ; Almidani, Omar ; Alvand, Saba ; Arabloo, Jalal u. a.: The global, regional, and national burden of urolithiasis in 204 countries and territories, 2000–2021: a systematic analysis for the Global Burden of Disease Study 2021. In: *EClinicalMedicine* 78 (2024)

[Aji23] Ajithkumar, Narayanan M.: *Enhancing Manipulation Performance with Grounded Haptic UI Teleoperation.* Aachen, Germany, RWTH Aachen University, Diplomarbeit, 2023. `https://elib.dlr.de/202109/1/Enhancing_Manipulation_Performance_with_Grounded_Haptic_UI_Teleoperation_Ajith.pdf`. – DLR Institute of Robotics and Mechatronics

[AJS+24] Akram, Mahir ; Jahrreiss, Victoria ; Skolarikos, Andreas ; Geraghty, Robert ; Tzelves, Lazaros ; Emilliani, Esteban ; Davis, Niall F. ; Somani, Bhaskar K.: Urological guidelines for kidney stones: overview and comprehensive update. In: *Journal of clinical medicine* 13 (2024), Nr. 4, S. 1114

[Ard] Arduino AG: *Arduino IDE.* https://www.arduino.cc/en/software, . – Accessed: 2025-11-14

[BCS+24] Bai, Junjie ; Chi, Yangjian ; Shangguan, Tong ; Lin, Jun ; Ye, Yushi ; Huang, Jianfeng ; Wen, Yahui ; Liu, Rong ; Chen, Ru ; Cai, Weizhong u. a.: Intrarenal pressure detection during flexible ureteroscopy with fiber optic pressure sensor system in porcine model. In: *Scientific Reports* 14 (2024), Nr. 1, S. 9446

[Ber23] Bergholz, Max: *Systematic review of haptic feedback in surgical robotics and factors affecting outcomes*, Technische Universität München, Diss., 2023

[BFW23] Bergholz, Max ; Ferle, Manuel ; Weber, Bernhard M.: The benefits of haptic feedback in robot assisted surgery and their moderators: a meta-analysis. In: *Scientific Reports* 13 (2023), Nr. 1, S. 19215

[Ble] Blender Foundation: *Blender.* https://www.blender.org/, . – Accessed: 2025-11-14

[BMB+25] Bhojani, Naeem ; Miller, Larry E. ; Bhattacharyya, Samir K. ; Chua, Wei J. ; Tailly, Thomas ; Eisner, Brian ; Chew, Ben H.: Continuous Intrarenal Pressure Monitoring during Endourological Procedures for Stone Disease: A Canary in the Coalmine for Optimizing Patient Safety. In: *Urologia Internationalis* (2025)

[BNV+19] Bjazevic, Jennifer ; Nott, Linda ; Violette, Philippe D. ; Tailly, Thomas ; Dion, Marie ; Denstedt, John D. ; Razvi, Hassan: The evolution of percutaneous nephrolithotomy: Analysis of a single institution experience over 25 years. In: *Canadian Urological Association Journal* 13 (2019), Nr. 10, S. E317

[BOL+08] Breda, Alberto ; Ogunyemi, Omolola ; Leppert, John T. ; Lam, John S. ; Schulam, Peter G.: Flexible ureteroscopy and laser lithotripsy for single intrarenal stones 2 cm or greater – is this the new frontier? In: *The Journal of Urology* 179 (2008), Nr. 3, 981–984. http://dx.doi.org/10.1016/j.juro.2007.10.075. – DOI 10.1016/j.juro.2007.10.075

[BS17] Bansal, P ; Sehgal, A: Expanding Indications of Flexible Ureteroscopy in Renal and Ureteral Stones. In: *J Urol Ren Dis: JURD-147. DOI* 10 (2017), S. 2575–7903

[ÇAT+25] Çavdar, OF ; Aydin, A ; Tokas, T ; Tozsin, A ; Gadzhiev, N ; Sönmez, MG ; Tekeli, R ; Ortner, G ; Kallidonis, P ; Akgül, B u. a.: Residual stone fragments: systematic review of definitions, diagnostic standards. In: *World Journal of Urology* 43 (2025), Nr. 1, S. 1–17

[CER+21] Campos, Carlos ; Elvira, Richard ; Rodríguez, Juan J G. ; Montiel, José MM ; Tardós, Juan D.: Orb-slam3: An accurate open-source library for visual, visual–inertial, and multimap slam. In: *IEEE transactions on robotics* 37 (2021), Nr. 6, S. 1874–1890

[Cho15] Cho, Sung Y.: Current status of flexible ureteroscopy in urology. In: *Korean Journal of Urology* 56 (2015), Nr. 10, 680–688. http://dx.doi.org/10.4111/kju.2015.56.10.680. – DOI 10.4111/kju.2015.56.10.680

[Coe] Coe, Fredric: *Treating Stones with Scopes and Lasers: Ureteroscopy.* https://kidneystones.uchicago.edu/2016/01/24/treating-stones-with-scopes-and-lasers-ureteroscopy/, . – Accessed: 2025-02-14

[DK24] Dagnino, Giulio ; Kundrat, Dennis: Robot-assistive minimally invasive surgery: trends and future directions. In: *International Journal of Intelligent Robotics and Applications* 8 (2024), Nr. 4, S. 812–826

[DMS+21] D'Ettorre, Claudia ; Mariani, Andrea ; Stilli, Agostino ; Baena, Ferdinando R. ; Valdastri, Pietro ; Deguet, Anton ; Kazanzides, Peter ; Taylor, Russell H. ; Fischer, Gregory S. ; DiMaio, Simon P. ; Menciassi, Arianna ; Stoyanov, Danail: Accelerating Surgical Robotics Research: A Review of 10 Years with the da Vinci Research Kit. In: *arXiv preprint* (2021). https://arxiv.org/pdf/2104.09869. – arXiv:2104.09869

[GBB+11] Gastrich, Michael D. ; Barone, Joseph ; Bachmann, Gary ; Anderson, Mark ; Balica, Adrian: Robotic surgery: review of the latest advances, risks, and outcomes. In: *Journal of Robotic Surgery* 5 (2011), June, Nr. 2, S. 79–97. http://dx.doi.org/10.1007/s11701-011-0246-y. – DOI 10.1007/s11701–011–0246–y. – Epub 2011 Jan 21

[GBD24] GBD 2021 Urolithiasis Collaborators: The global, regional, and national burden of urolithiasis in 204 countries and territories, 2000–2021: a systematic analysis for the Global Burden of Disease Study 2021. In: *EClinicalMedicine* 78 (2024), 102924. http://dx.doi.org/10.1016/j.eclinm.2024.102924. – DOI 10.1016/j.eclinm.2024.102924

[GIS+25] Gopi, Praveen ; Ishfaq, Muhammed ; Shkoukani, Zakaria W. ; Awsare, Ninaad ; McCabe, John ; Samsudin, Azi ; Hughes, Kaylie E. ; Abdulmajed, Mohamed: Robotic Flexible Ureteroscopy: Systematic Review and Meta-Analysis of Surgical Efficacy, Safety and Ergonomic Outcomes. In: *Cureus* 17 (2025), Nr. 8

[HCB14] He, Ding S. ; Ciavarella, David J. ; Burnside, Eddie K.: *Bioimpedance-*

assisted placement of a medical device. August 12 2014. – US Patent 8,801,693

[HDC+24] He, Min ; Dong, Yonghui ; Cai, Wansong ; Cai, Jiale ; Xie, Yaming ; Yu, Mingke ; Li, Changjiu ; Wen, Liping: Recent advances in the treatment of renal stones using flexible ureteroscopys. In: *International Journal of Surgery* 110 (2024), Nr. 7, S. 4320–4328

[HHBH+24] Henderickx, Michaël MEL ; Hendriks, Nora ; Bouma-Houwert, A C. ; Baard, Joyce ; Kamphuis, Guido M. ; Schuil, Hugo W. ; Beerlage, Harrie P. ; Bruin, D M.: Heavy as a rock or light as dust: a comparison between the perceived workload for extracorporeal shockwave lithotripsy, ureterorenoscopy and percutaneous nephrolithotomy. In: *Central European journal of urology* 77 (2024), Nr. 1, S. 129

[HPC+11] Healy, Kelly A. ; Pak, Raymond W. ; Cleary, Ryan C. ; Colon-Herdman, Arturo ; Bagley, Demetrius H.: Hand problems among endourologists. In: *Journal of endourology* 25 (2011), Nr. 12, S. 1915–1920

[ImF] ImFusion GmbH: *ImFusion Suite: Visual Computing for Medical Imaging.* `https://imfusion.com/products-overview/imfusion-suite/`, . – Accessed: 2025-11-14

[Int23] Intuitive Surgical Operations, Inc.: *da Vinci Vision: Enhancing visualization.* `https://www.intuitive.com/en-us/products-and-services/da-vinci/vision`, 2023. – Accessed: 2025-11-14

[Int25] Intuitive Surgical Operations, Inc.: *da Vinci 5: Our most advanced and integrated robotic surgery system–ever.* `https://www.intuitive.com/en-us/products-and-services/da-vinci/5`, 2025. – Accessed: 2025-11-14

[KJM+22] Kim, Joonhwan ; Jung, Hae D. ; Moon, Young J. ; Han, Hyunho ; Cheon, Byungsik ; Han, Jungmin ; Cho, Sung Y. ; Lee, Joo Y. ; Kwon, Dong S.: In Vivo Feasibility Test of a New Flexible Ureteroscopic Robotic System, *easyUretero*, for Renal Stone Retrieval in a Porcine Model. In: *Yonsei Medical Journal* 63 (2022), Nr. 12, S. 1106–1112. `http://dx.doi.org/10.3349/ymj.2022.0367`. – DOI 10.3349/ymj.2022.0367

[KO22] Kezer, Cem ; Ozgor, Faruk: Defining the Learning Curve of Flexible Ureterorenoscopy and Laser Lithotripsy. In: *Urol Journal* 20 (2022), December, Nr. 1, S. 7–10. `http://dx.doi.org/10.22037/uj.v19i.7389`. – DOI 10.22037/uj.v19i.7389. – Epub 2022 Dec 25

[KPL13] Kaduk, Wolfram M. ; Podmelle, Fred ; Louis, Patrick J.: Surgical navigation in reconstruction. In: *Oral and Maxillofacial Surgery Clinics* 25 (2013), Nr. 2, S. 313–333

[KSHK+21a] Klodmann, Julian ; Schlenk, Christopher ; Hellings-Kuss, Anja ; Bahls, Thomas ; Unterhinninghofen, Roland ; Albu-Schäffer, Alin O. ; Hirzinger, Gerhard: An Introduction to Robotically Assisted Surgical Systems: Current Developments and Focus Areas of Research. In: *Current Robotics Reports* 2 (2021), Nr. 3, S. 321–332. http://dx.doi.org/10.1007/s43154-021-00064-3. – DOI 10.1007/s43154–021–00064–3. – ISSN 2662–4087

[KSHK+21b] Klodmann, Julian ; Schlenk, Christopher ; Hellings-Kuss, Anja ; Bahls, Thomas ; Unterhinninghofen, Roland ; Albu-Schäffer, Alin ; Hirzinger, Gerd: An Introduction to Robotically Assisted Surgical Systems: Current Developments and Focus Areas of Research. In: *Current Robotics Reports* 2 (2021), Nr. 3, 321–332. http://dx.doi.org/10.1007/s43154-021-00064-3. – DOI 10.1007/s43154–021–00064–3. – ISSN 2662–4087

[LDMFD24] Lai, Chun-Feng ; De Momi, Elena ; Ferrigno, Giancarlo ; Dankelman, Jenny: Using a Guidance Virtual Fixture on a Soft Robot to Improve Ureteroscopy Procedures in a Phantom. In: *Robotics* 13 (2024), Nr. 9, S. 140

[LGF+23] Lin, Jialin ; Guo, Xiaoqing ; Fan, Wen ; Li, Wei ; Wang, Yuanyi ; Liang, Jiaming ; Liu, Weiru ; Wei, Lei ; Zhang, Dandan: *TIMS: A Tactile Internet-Based Micromanipulation System with Haptic Guidance for Surgical Training*. arXiv preprint arXiv:2303.03566. https://arxiv.org/abs/2303.03566. Version: 2023. – Preprint — not peer-reviewed

[LJ22] Lee, Joo Y. ; Jeon, Seung H.: Robotic Flexible Ureteroscopy: A New Challenge in Endourology. In: *Investigative and Clinical Urology* 63 (2022), Nr. 5, S. 483–485. http://dx.doi.org/10.4111/icu.20220256. – DOI 10.4111/icu.20220256

[LJ25] Lykkegaard, Emmeli G. ; Jung, Helene: Intrarenal pressure during ureteroscopy. In: *European Urology Focus* (2025)

[LLY23] Lin, Zhefan ; Lei, Chen ; Yang, Liangjing: Modern image-guided surgery: a narrative review of medical image processing and visualization. In: *Sensors* 23 (2023), Nr. 24, S. 9872

[MCC+22] Machaca, Sergio ; Cao, Eric ; Chi, Amy ; Adrales, Gina ; Kuchenbecker, Katherine J. ; Brown, Jeremy D.: Wrist-Squeezing Force Feedback Improves Accuracy and Speed in Robotic Surgery Training. In: *arXiv* *preprint arXiv:2205.06927* (2022). http://dx.doi.org/10.48550/arXiv.2205.06927. – DOI 10.48550/arXiv.2205.06927

[Mes] Visual Computing Lab, ISTI–CNR: *MeshLab*. https://www.meshlab.net/, . – Accessed: 2025-11-14

[MHP+20] McCahy, Philip J. ; Hong, Matthew ; Paul, Eldho ; Berman, Ivor ; Shahbaz, Shekib: Shock-wave lithotripsy, ureterorenoscopy and percutaneous nephrolithotomy for 1–2 cm renal stones: a randomised pilot study. In: *Journal of Clinical Urology* 13 (2020), Nr. 6, S. 413–418

[MRK+24] Marcus, Hani J. ; Ramirez, Pedro T. ; Khan, Danyal Z. ; Layard Horsfall, Hugo ; Hanrahan, John G. ; Williams, Simon C. ; Beard, David J. ; Bhat, Rani ; Catchpole, Ken ; Cook, Andrew u. a.: The IDEAL framework for surgical robotics: development, comparative evaluation and long-term monitoring. In: *Nature medicine* 30 (2024), Nr. 1, S. 61–75

[NGBS+23] Nobbenhuis, Marielle A. E. ; Gul, Nahid ; Barton-Smith, Peter ; O'Sullivan, Orfhlaith ; Moss, Esther ; Ind, Thomas E. J. ; Obstetricians, Royal C. ; Gynaecologists: Robotic surgery in gynaecology: Scientific Impact Paper No. 71 (July 2022). In: *BJOG: An International Journal of Obstetrics and Gynaecology* 130 (2023), Nr. 1, S. e1–e8. http://dx.doi.org/10.1111/1471-0528.17242. – DOI 10.1111/1471–0528.17242. – Epub 2022 Jul 17

[Oka04] Okamura, Allison M.: Methods for Haptic Feedback in Teleoperated Robot-Assisted Surgery. In: *Industrial Robot* 31 (2004), Nr. 6, 499–508. http://dx.doi.org/10.1108/01439910410566362. – DOI 10.1108/01439910410566362

[Oka09] Okamura, Allison M.: Haptic feedback in robot-assisted minimally invasive surgery. In: *Current opinion in urology* 19 (2009), Nr. 1, S. 102–107

[OMSK+23] Oliva Maza, Laura ; Steidle, Florian ; Klodmann, Julian ; Strobl, Klaus ; Triebel, Rudolph: An ORB-SLAM3-based approach for surgical navigation in ureteroscopy. In: *Computer Methods in Biomechanics and Biomedical Engineering: Imaging & Visualization* 11 (2023), Nr. 4, S. 1005–1011

[PBCV24] Pauchard, F ; Bhojani, N ; Chew, B ; Ventimiglia, E: How to measure intra-renal pressure during flexible URS: Historical background, technological innovations and future perspectives. In: *Actas Urológicas Españolas (English Edition)* 48 (2024), Nr. 1, S. 42–51

[PGS24] Pozdzik, Agnieszka ; Grillo, Viridiana ; Sakhaee, Khashayar: Gaps in kidney stone disease management: From clinical theory to patient reality. In: *Urolithiasis* 52 (2024), Nr. 1, S. 61. http://dx.doi.org/10.1007/s00240-024-01563-6. – DOI 10.1007/s00240–024–01563–6. – Published 9 April 2024

[PNL+24] Picozzi, Paola ; Nocco, Umberto ; Labate, Chiara ; Gambini, Isabella ; Puleo, Greta ; Silvi, Federica ; Pezzillo, Andrea ; Mantione, Rocco ; Cimolin, Veronica: Advances in robotic surgery: a review of new surgical platforms. In: *Electronics* 13 (2024), Nr. 23, S. 4675

[RAA10] Romero, Victoriano ; Akpinar, Haluk ; Assimos, Dean G.: Kidney stones: a global picture of prevalence, incidence, and associated risk factors. In: *Reviews in urology* 12 (2010), Nr. 2-3, S. e86

[RAP+08] Rajamahanty, S. ; Anderson, J. K. ; Plante, M. K. ; Chan, P. T. ; Baldwin, D. D.: Flexible ureteroscopy update: indications, instrumentation and technique. In: *Indian Journal of Urology* 24 (2008), Nr. 4, 532–537. https://pdfs.semanticscholar.org/1e85/a8019ae65dd463e453ca90eb9d5f997ee55d.pdf

[ROS25] ROS (ROS Development Team / Open Source Robotics Foundation): *ROS Wiki*. https://wiki.ros.org/, 2025. – Accessed: 2025-11-14

[RSC+15] Rex, Douglas K. ; Schoenfeld, Philip S. ; Cohen, Jonathan ; Pike, Irving M. ; Adler, Douglas G. ; Fennerty, Brian M. ; Lieb, John G. ; Park, Walter G. ; Rizk, Maged K. ; Sawhney, Mandeep S. u. a.: Quality indicators for colonoscopy. In: *Official journal of the American College of Gastroenterology| ACG* 110 (2015), Nr. 1, S. 72–90

[RSHK+22] Rassweiler-Seyfried, Marie-Claire ; Herrmann, Jonas ; Klein, Jan ; Michel, Maurice-Stephan ; Rassweiler, Jens ; Grüne, Britta: Robot-assisted flexible ureterorenoscopy: state of the art in 2022. In: *Mini-invasive Surg* 6 (2022), S. 41

[RVi] ROS (Open Source Robotics Foundation / ROS Development Team): *RViz – 3D Robot Visualizer for ROS*. https://wiki.ros.org/rviz, . – Accessed: 2025-11-14

[Sal05] Salameh, F.: A New Device to Clarify the Position of the Endoscope Tip during Endoscopic Diagnosis and Therapeutic Procedures. In: *Endoscopy* 37 (2005), Nr. 3, S. 278. http://dx.doi.org/10.1055/s-2005-861014. – DOI 10.1055/s–2005–861014

[SDA24] Selim, Mostafa ; Dresscher, Douwe ; Abayazid, Momen: A comprehensive review of haptic feedback in minimally invasive robotic liver surgery:

advancements and challenges. In: *The International Journal of Medical Robotics and Computer Assisted Surgery* 20 (2024), Nr. 1, S. e2605

[SDE+25] Somani, Bhaskar ; Davis, Niall ; Emiliani, Esteban ; Göcke, Mehmet I. ; Jung, Helene ; Keller, Etienne X. ; Miernik, Arkadiusz ; Proietti, Silvia ; Turney, Ben ; Wiseman, Oliver u. a.: Intrarenal pressure monitoring during ureteroscopy: a delphi panel consensus. In: *European Urology Open Science* 73 (2025), S. 43–50

[SGT+23] Sinha, Mriganka M. ; Gauhar, Vineet ; Tzelves, Lazaros ; Tefik, Tzevat ; Ergul, Rifat B. ; Juliebø-Jones, Patrick ; Somani, Bhaskar K.: Technical Aspects and Clinical Outcomes of Robotic Ureteroscopy: Is It Ready for Primetime? In: *Current Urology Reports* 24 (2023), August, Nr. 8, S. 391–400. http://dx.doi.org/10.1007/s11934-023-01167-4. – DOI 10.1007/s11934–023–01167–4. – Epub 2023 Jun 1

[SHS+23] Schlenk, Christopher ; Hagmann, Katharina ; Steidle, Florian ; Oliva Maza, Laura ; Kolb, Alexander ; Hellings-Kuss, Anja ; Schöb, Dominik S. ; Klodmann, Julian ; Miernik, Arkadiusz ; Albu-Schäffer, Alin: A robotic system for solo surgery in flexible ureteroscopy: development and evaluation with clinical users. In: *International journal of computer assisted radiology and surgery* 18 (2023), Nr. 9, S. 1559–1569

[SHW+22] Shu, Xiongpeng ; Hua, Peng ; Wang, Shuang ; Zhang, Ling ; Xie, Le: Safety enhanced surgical robot for flexible ureteroscopy based on force feedback. In: *The International Journal of Medical Robotics and Computer Assisted Surgery* 18 (2022), Nr. 5, S. e2410

[TC13] Tefekli, Ahmet ; Cezayirli, Fatin: The history of urinary stones: in parallel with civilization. In: *The Scientific World Journal* 2013 (2013), Nr. 1, S. 423964

[TMW+17a] Talari, Hadi F. ; Monfaredi, Reza ; Wilson, Emmanuel ; Blum, Emily ; Bayne, Christopher ; Peters, Craig ; Zhang, Anlin ; Cleary, Kevin: Robotically assisted ureteroscopy for kidney exploration. In: *Proceedings of SPIE — International Society for Optical Engineering* 10135 (2017), S. 1013512. http://dx.doi.org/10.1117/12.2253862. – DOI 10.1117/12.2253862. – Epub 2017 Mar 3

[TMW+17b] Talari, Hadi F. ; Monfaredi, Reza ; Wilson, Emmanuel ; Blum, Emily ; Bayne, Christopher ; Peters, Craig ; Zhang, Anlin ; Cleary, Kevin: Robotically assisted ureteroscopy for kidney exploration. In: *Proceedings of Spie–the International Society for Optical Engineering* Bd. 10135, 2017, S. 1013512

[Uni25] University of Washington Pressbooks: *Urinary System Anatomy – Kidney Collecting System.* https://uw.pressbooks.pub/pbio375/chapter/urinary-system-anatomy/, 2025. – In *Human Physiology in Health and Disease.* Creative Commons License.

[Wis22] Wiseman, Oliver: *Evolving Trends Lead to Unmet Needs in Flexible Ureteroscopy.* Online article. https://www.bostonscientific.com/en-US/medical-specialties/urology/stonesmart/smarthub/evolving-trends-lead-to-unmet-needs-in-flexible-ureteroscopy.html. Version: Juni 2022. – Accessed: 2025-11-13

[WL24] Wason, Shaun E. ; Leslie, Stephen W.: Ureteroscopy. Version: 2024. https://www.ncbi.nlm.nih.gov/books/NBK560556/. In: *StatPearls.* Treasure Island, FL : StatPearls Publishing, 2024. – Available from: StatPearls [Internet]

[WZZ+21] Wang, Zhu ; Zhang, Ying ; Zhang, Jianwen ; Deng, Qiong ; Liang, Hui: Recent advances on the mechanisms of kidney stone formation. In: *International journal of molecular medicine* 48 (2021), Nr. 2, S. 149

[YCY+25] Yuen, Steffi Kar K. ; Chen, Zixiao ; Yuen, Skyler ; Liu, Alex Q. ; Leung, Chi-Ho ; Ko, Ivan Ching H. ; Chan, Chi K. ; Somani, Bhaskar ; Herrmann, Thomas ; Jung, Helene u. a.: Novel non-invasive intrarenal pressure monitoring devices in flexible ureteroscopy: an in-vitro comparative study. In: *World Journal of Urology* 43 (2025), Nr. 1, S. 1–8

[YKT+14a] Yoshida, Kenji ; Kawa, Gen ; Taniguchi, Hisanori ; Inoue, Takaaki ; Mishima, Takao ; Yanishi, Masaaki ; Sugi, Motohiko ; Kinoshita, Hidefumi ; Matsuda, Tadashi: Novel ureteroscopic navigation system with a magnetic tracking device: a preliminary ex vivo evaluation. In: *Journal of Endourology* 28 (2014), September, Nr. 9, S. 1053–1057. http://dx.doi.org/10.1089/end.2013.0757. – DOI 10.1089/end.2013.0757

[YKT+14b] Yoshida, Kenji ; Kawa, Gen ; Taniguchi, Hisanori ; Inoue, Takaaki ; Mishima, Takumi ; Yanishi, Masafumi ; Sugi, Motohiko ; Kinoshita, Hidefumi ; Matsuda, Tadashi: Novel Ureteroscopic Navigation System with a Magnetic Tracking Device: A Preliminary Ex Vivo Evaluation. In: *Journal of Endourology* 28 (2014), Nr. 9, S. 1053–1057. http://dx.doi.org/10.1089/end.2013.0757. – DOI 10.1089/end.2013.0757

[YYM+15] Yoshida, Kenji ; Yokomizo, Akira ; Matsuda, Tadashi ; Hamasaki, Takuya ; Kondo, Yusuke ; Yamaguchi, Kunihisa ; Kanayama, Hiro-omi ; Wakumoto, Yasuhisa ; Horie, Shinya ; Naito, Seiji: The Advantage of a Ureteroscopic Navigation System with Magnetic Tracking in Comparison with Simulated Fluoroscopy in a Phantom Study. In: *Journal of Endourology*

29 (2015), Nr. 9, S. 1059–1064. http://dx.doi.org/10.1089/end.2015.0054. – DOI 10.1089/end.2015.0054

[ZZP+22] ZHANG, Lu ; ZHANG, Xu ; PU, Yuanchun ; ZHANG, Yaodong ; FAN, Jinhai: Global, regional, and national burden of urolithiasis from 1990 to 2019: a systematic analysis for the global burden of disease study 2019. In: *Clinical Epidemiology* (2022), S. 971–983